Neuron
Article

Accumulation of AMPA Receptors in Autophagosomes in Neuronal Axons Lacking Adaptor Protein AP-4

Shinji Matsuda,[1] Eriko Miura,[2] Keiko Matsuda,[1] Wataru Kakegawa,[1] Kazuhisa Kohda,[1] Masahiko Watanabe,[2] and Michisuke Yuzaki[1,*]
[1]Department of Physiology, School of Medicine, Keio University, Tokyo 160-8582, Japan
[2]Department of Anatomy, Hokkaido University School of Medicine, Sapporo 060-8638, Japan
*Correspondence: myuzaki@a5.keio.jp
DOI 10.1016/j.neuron.2008.02.012

SUMMARY

AP-4 is a member of the adaptor protein complexes, which control vesicular trafficking of membrane proteins. Although AP-4 has been suggested to contribute to basolateral sorting in epithelial cells, its function in neurons is unknown. Here, we show that disruption of the gene encoding the β subunit of AP-4 resulted in increased accumulation of axonal autophagosomes, which contained AMPA receptors and transmembrane AMPA receptor regulatory proteins (TARPs), in axons of hippocampal neurons and cerebellar Purkinje cells both in vitro and in vivo. AP-4 indirectly associated with the AMPA receptor via TARPs, and the specific disruption of the interaction between AP-4 and TARPs caused the mislocalization of endogenous AMPA receptors in axons of wild-type neurons. These results indicate that AP-4 may regulate proper somatodendritic-specific distribution of its cargo proteins, including AMPA receptor-TARP complexes and the autophagic pathway in neurons.

INTRODUCTION

Membrane proteins reach their resident organelles and plasma membrane domains by vesicle carriers that selectively sort cargo proteins. Four tetrameric adaptor protein (AP) complexes, AP-1, AP-2, AP-3, and AP-4, have been shown to control vesicular trafficking of membrane proteins in the biosynthetic and endocytic pathways (Boehm and Bonifacino, 2001). The most recently described member, AP-4, is associated with the trans-Golgi network (TGN) and/or endosomes (Barois and Bakke, 2005) and has been shown to mediate basolateral sorting of its cargo proteins via the biosynthetic pathway in epithelial cells (Folsch et al., 1999; Simmen et al., 2002); when AP-4 was disrupted, basolaterally transported proteins, such as low-density lipoprotein receptors (LDLR), were distributed nonselectively to both basolateral and apical domains. Similarly, AP-4 is expressed in the TGN and endosomes in neuronal cell lines (Dilaver et al., 2003) and in many regions of the brain (Yap et al., 2003) (The Allen Brain Atlas, http://www.brain-map.org). Nevertheless, its functions and endogenous cargo proteins are unknown in neurons.

Like epithelial cells, neurons are highly polarized cells composed of two morphologically and functionally distinct domains, the axon and the dendrite. Once neuronal processes are destined to become axons or dendrites during development, neuronal polarity is maintained throughout adulthood by the selective sorting of many membrane proteins, such as ion channels, receptors, transporters, and adhesion molecules, to their proper locations. Indeed, the AMPA receptor, which mainly mediates fast excitatory neurotransmission in the vertebrate CNS, is selectively transported to the somatodendritic domain in neurons (Horton and Ehlers, 2003). Dendrite-selective sorting often requires a short stretch of amino acids, such as a dileucine (Poyatos et al., 2000; Rivera et al., 2003; Silverman et al., 2005) or tyrosine-based motif (Jareb and Banker, 1998), within the cytosolic domain of the membrane protein to be sorted. Similarly, the C-terminal cytoplasmic tail of the GluR1 subunit of AMPA receptors was shown to contain dendritic sorting information, which did not rely on a dileucine or tyrosine-based motif (Ruberti and Dotti, 2000). Interestingly, proteins sorted to the basolateral domain of epithelial cells are often (Dotti and Simons, 1990; Jareb and Banker, 1998), but not always (Silverman et al., 2005), selectively transported to the somatodendritic domain of neurons. Thus, a common mechanism may be involved in polarized sorting in neuronal and epithelial cells.

In this study, to elucidate the role of AP-4 in neurons, we disrupted the gene encoding the β subunit of AP-4 (*AP-4*$\beta^{-/-}$). Although *AP-4*$\beta^{-/-}$ mice were fertile and had no overt anatomical and gait abnormalities, the axon terminal regions of *AP-4*$\beta^{-/-}$ Purkinje cells and hippocampal neurons were swollen and contained numerous autophagosomes, which were immunopositive for AMPA receptors and transmembrane AMPA receptor regulatory proteins (TARPs). Although AP-4 did not directly bind to AMPA receptors, it did associate with TARPs, which tightly binds to all subunits of AMPA receptors GluR1–GluR4 (Nicoll et al., 2006). Indeed, the specific disruption of the interaction between AP-4 and TARPs caused the mislocalization of endogenous AMPA receptors in the axons of wild-type neurons. These results indicate that AP-4 regulates proper somatodendritic-specific distribution of its cargo proteins, including AMPA receptor-TARP complexes and the autophagic pathway in neurons.

RESULTS

Generation of *AP-4*$\beta^{-/-}$ Mice

To investigate the role of AP-4 in neurons in vivo, we analyzed mice carrying a null mutation in the gene encoding the β4

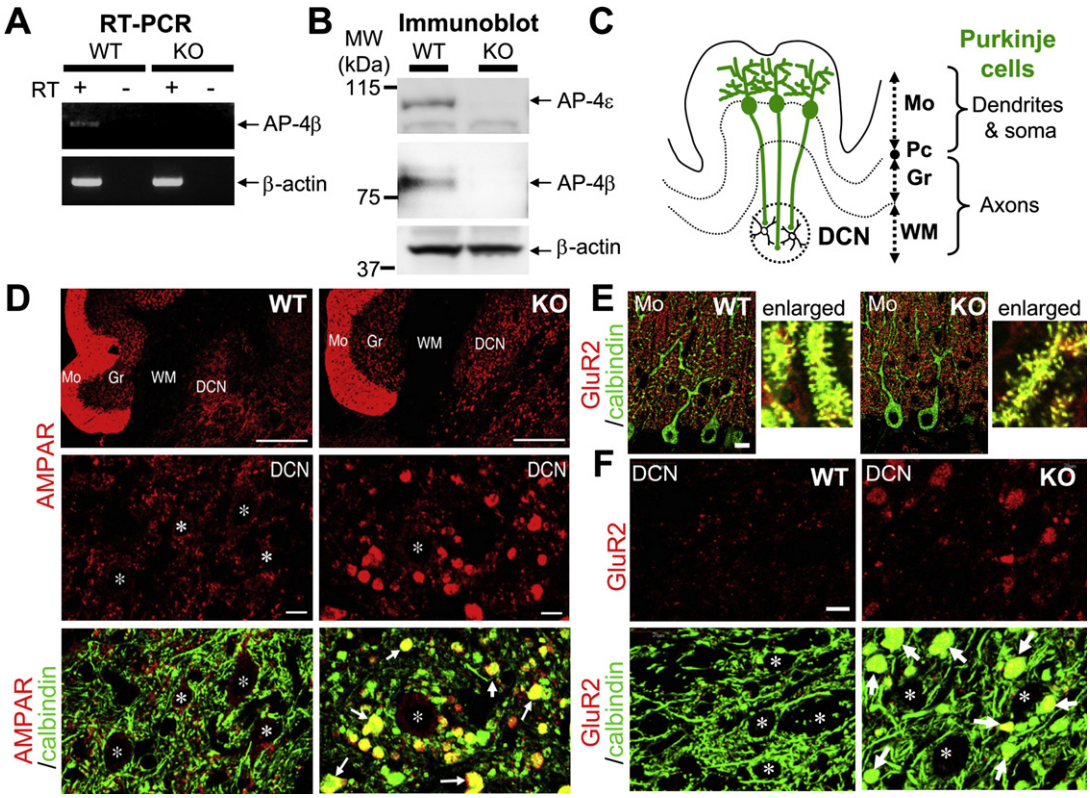

Figure 1. Accumulation of AMPA Receptors in Purkinje Cell Axons in the DCN Region of *AP-4β*$^{-/-}$ Cerebellum In Vivo

(A) PCR analysis using total RNAs from wild-type (WT) and *AP-4β*$^{-/-}$ (KO) brain tissues with or without treatment with reverse transcriptase (RT).

(B) Immunoblot analysis of whole-brain lysates from wild-type and *AP-4β*$^{-/-}$ mice using anti-AP-4ε (top), anti-AP-4β (middle), or anti-β-actin (bottom) antibodies.

(C) Schematic illustration of laminated cortical structure of the cerebellum. Purkinje cell axons converge on the deep cerebellar nucleus (DCN). Mo, molecular layer; Pc, Purkinje cell layer; Gr, granular layer; WM, white matter.

(D) Immunohistochemical analysis of AMPA receptors (red) and calbindin (green) localization in wild-type and *AP-4β*$^{-/-}$ cerebella. The lower four panels represent enlarged images of the DCN region. The asterisks indicate the soma of DCN neurons, and the arrows indicate the axons of Purkinje cells, which are doubly immunopositive for calbindin and AMPA receptors. Scale bars correspond to 200 μm in the upper panels, 10 μm in the lower panels.

(E) Immunohistochemical analysis of AMPA receptor GluR2 subunit (red) and calbindin (green) localization in the molecular layer (Mo) of wild-type and *AP-4β*$^{-/-}$ cerebella. GluR2 was normally distributed in the dendrites of Purkinje cells (enlarged in the right panels). Scale bar, 20 μm.

(F) Immunohistochemical analysis of AMPA receptor GluR2 subunit (red) and calbindin (green) localization in the DCN region of wild-type and *AP-4β*$^{-/-}$ cerebella. The asterisks indicate the soma of DCN neurons, and the arrows indicate the axons of Purkinje cells, which are doubly immunopositive for calbindin and GluR2. Scale bar, 10 μm.

subunit, a large subunit of AP-4. The disruption of the β4 gene was confirmed by Southern blot and polymerase chain reaction (PCR) analyses of genomic DNA (see Figure S1 available online). Similarly, no normal β4 mRNA was detected in brain tissue from *AP-4β*$^{-/-}$ mice using reverse transcriptase PCR (Figure 1A). Immunoblot analysis of brain lysates with anti-β4 antibody also detected no AP-4β proteins in *AP-4β*$^{-/-}$ mice (Figure 1B). The ablation of one of the four subunits of an AP complex generally results in the total loss of function of the AP complex in mammals and other eukaryotes (Dell'Angelica et al., 1999; Kantheti et al., 1998). Indeed, immunoblot analysis revealed that the expression of the ε subunit, another large subunit of AP-4, was barely detectable in *AP-4β*$^{-/-}$ mice (Figure 1B).

Although a null mutation in the genes encoding the subunits of AP-1 or AP-2 results in embryonic lethality in homozygous mice (Boehm and Bonifacino, 2001), heterozygous *AP-4β* breeding pairs produced normal litters (128 pups, 52% female) with the expected frequencies of wild-type, heterozygous, and homozygous offspring (22%, 55%, and 23%, respectively). *AP-4β*$^{-/-}$ mice were fertile, had no overt anatomical abnormalities in their brains (Figure S2), and had normal life spans. Although the mice exhibited no ataxia and could walk along a straight line with regular steps (Figure S3A), they exhibited a significantly poorer rotorod performance than wild-type mice (Figure S3B). No significant differences in body weight or grip power were observed between the wild-type and *AP-4β*$^{-/-}$ mice (Figures S3C and S3D). In addition, the cerebella of the *AP-4β*$^{-/-}$ mice had normal foliation and a normal laminated cortical structure (Figure S3E). All the principal neuronal types were present in the cerebella (Figure S3E), and the gross morphology of the soma and dendrites of Purkinje cells was normal (Figure S3F) in the *AP-4β*$^{-/-}$ mice. Since AP-4 is expressed in many regions of the brain (Yap et al., 2003; The Allen Brain Atlas, http://www.brain-map.org) and disruption of *AP-4β* had effects on various neurons as

described below, neurons directly responsible for the poor motor performance of *AP-4β*$^{-/-}$ mice remains unclear; future studies using the brain region-specific knockout of the *AP-4* gene are warranted.

Mislocalization of AMPA Receptors in *AP-4β*$^{-/-}$ Purkinje Cells

Because AP-4 mediates basolateral sorting of cargo proteins in epithelial cells (Folsch et al., 1999; Simmen et al., 2002), we examined whether the polarized distribution of AMPA receptors to the somatodendritic domain, a functional equivalent of the basolateral domain of epithelial cells, was disrupted in *AP-4β*$^{-/-}$ neurons. Purkinje cells provide an excellent model system to study protein sorting in vivo because their dendritic field is spatially segregated from their axonal field (Figure 1C; Mitsui et al., 2005). Purkinje cells extend elaborate dendrites into the molecular layer and project a single axon, in the opposite direction, into the deep cerebellar nuclei (DCN); since Purkinje cells are the only calbindin-positive cells in the cerebellum, the axons of Purkinje cells in the DCN region can be easily identified. In wild-type and *AP-4β*$^{-/-}$ mice, AMPA receptor immunoreactivities were mainly observed in the molecular layer of the cerebellum, with lower levels observed in the granular layer and DCN (Figure 1D). Magnified images of the DCN region of wild-type cerebella revealed that AMPA receptor immunoreactivity was not colocalized with the axons of Purkinje cells, which were visualized using anti-calbindin antibody (Figure 1D); this result indicated that AMPA receptors in wild-type Purkinje cells were selectively transported to the somatodendritic domain. In contrast, AMPA receptor immunoreactivity around the DCN of *AP-4β*$^{-/-}$ cerebella was localized in huge bulging structures that were immunopositive for calbindin (Figure 1D). Similar results were obtained from immunohistochemical analyses using specific antibodies against the GluR1 (Figure S4A) and GluR2 (Figures 1E and 1F) subunits of AMPA receptors. On the other hand, GluR2 immunoreactivity in the molecular layer of *AP-4β*$^{-/-}$ cerebella displayed normal punctate patterns that corresponded to the Purkinje cell spines (Figure 1E), suggesting that the transport of AMPA receptors to the dendrites was intact in *AP-4β*$^{-/-}$ Purkinje cells.

To confirm that the bulging structures were, indeed, the axons of Purkinje cells, immunohistochemical analyses were performed using anti-tau1 and anti-MAP2 antibodies, which specifically recognize axons and somatodendritic regions, respectively. Strong tau1 and calbindin immunoreactivities were colocalized in the bulging structures in the DCN region of *AP-4β*$^{-/-}$ cerebella, while MAP2 immunoreactivity was barely detectable (Figure 2A). We confirmed that the anti-tau1 antibody did not react with the soma and dendrites of either wild-type or *AP-4β*$^{-/-}$ Purkinje cells (Figure 2B); tau1 immunoreactivity in the molecular layer corresponded to axons of granule cells that formed synapses on Purkinje-cell dendrites. Thus, the bulging structures in the DCN were most likely the axons of Purkinje cells. In addition, we used patch pipettes to introduce Alexa dye directly into *AP-4β*$^{-/-}$ Purkinje cells and found that Alexa-filled axons in the DCN region were swollen and immunopositive for AMPA receptors and calbindin (Figure S5). Furthermore, cultured Purkinje cells from *AP-4β*$^{-/-}$ mice, but not from wild-type mice, also displayed swollen axons with localized AMPA receptor immunoreactivity (Figure 2C). Interestingly, the AMPA receptors had accumulated at or near the axonal terminal regions, but not in thin axonal shafts (Figure 2C); this result may explain why some calbindin-positive regions, which probably corresponded to the axonal shafts, were immunonegative for AMPA receptors in the DCN region of *AP-4β*$^{-/-}$ mice (Figure 1D). Altogether, these results indicate that AMPA receptors were mislocalized and accumulated at or near the axon terminals of *AP-4β*$^{-/-}$ Purkinje cells.

Axon transport is disturbed in a variety of neurological diseases as well as in traumatic, toxic, or ischemic injuries, leading to localized axonal swelling. For example, we recently demonstrated that the Purkinje cell-specific knockout of *Atg5*, an autophagy-related gene necessary for the elongation of the isolation membrane, resulted in marked axon swelling before the Purkinje cells started to degenerate (Nishiyama et al., 2007). However, immunoreactivity for AMPA receptors did not accumulate in the swollen calbindin-positive Purkinje cell axons in *Atg5* null cerebella (Figure 2D). Furthermore, unlike AMPA receptors, metabotropic glutamate receptor 1 (mGluR1) showed highly polarized distribution in the somatodendritic regions of both wild-type and *AP-4β* KO Purkinje cells; mGluR1 immunoreactivity was not colocalized with calbindin immunoreactivity in the DCN region of cerebella (Figure S4B), and it was restricted to the somatodendritic domain of Purkinje cells (Figure S4C). These results indicate that the lack of AP-4 did not cause nonspecific detrimental effects on Purkinje cells but that AP-4 is required for the somatodendritic domain-specific distribution of AMPA receptors in Purkinje cells in vivo.

Accumulation of AMPA Receptors in Autophagosomes in Axons of Purkinje Cells

Electron microscopy analysis revealed membranous organelles, including vesicles, vacuoles, stacked endoplasmic reticulum (ER), and autophagosome-like structures, highly accumulated in the bulging portions of axons (shown by # in Figures 3A-2, 3A-4, and 3A-5), which were several times larger in size than the Purkinje cell axons in wild-type cerebella (Figures 3A-1 and 3A-3). Occasionally, membranous organelles also accumulated in the axon terminals that formed synapses with DCN neurons (Figure 3A-5). Similarly, electron microscopy frequently revealed swollen and aberrant axons of cerebellar granule neurons in *AP-4β*$^{-/-}$ cerebella (Figure 3B), a finding consistent with the view that AP-4 plays a role in various neurons. In contrast, synaptic vesicle-accumulating axon terminals in the *AP-4β*$^{-/-}$ cerebella were mostly similar in size to those in wild-type cerebella, and these terminals formed normal synapses (thick arrows in Figure 3A) with the DCN neurons. Moreover, the density of Purkinje cell axon terminals, which were identified by the immunoreactivity of vesicular GABA transporter (VGAT) and calbindin, were not different in the *AP-4β*$^{-/-}$ DCN regions from that in wild-type DCN regions (Figure S6). Thus, the presence of abundant aberrant structures may not significantly affect the function of axon terminals.

To obtain clues to the identity of autophagosome-like structures, we performed immunoblotting analysis with anti-microtubule associated protein light chain 3 (LC3) antibody; a lipidated form of LC3, LC3-II, has been shown to be a specific autophagosomal

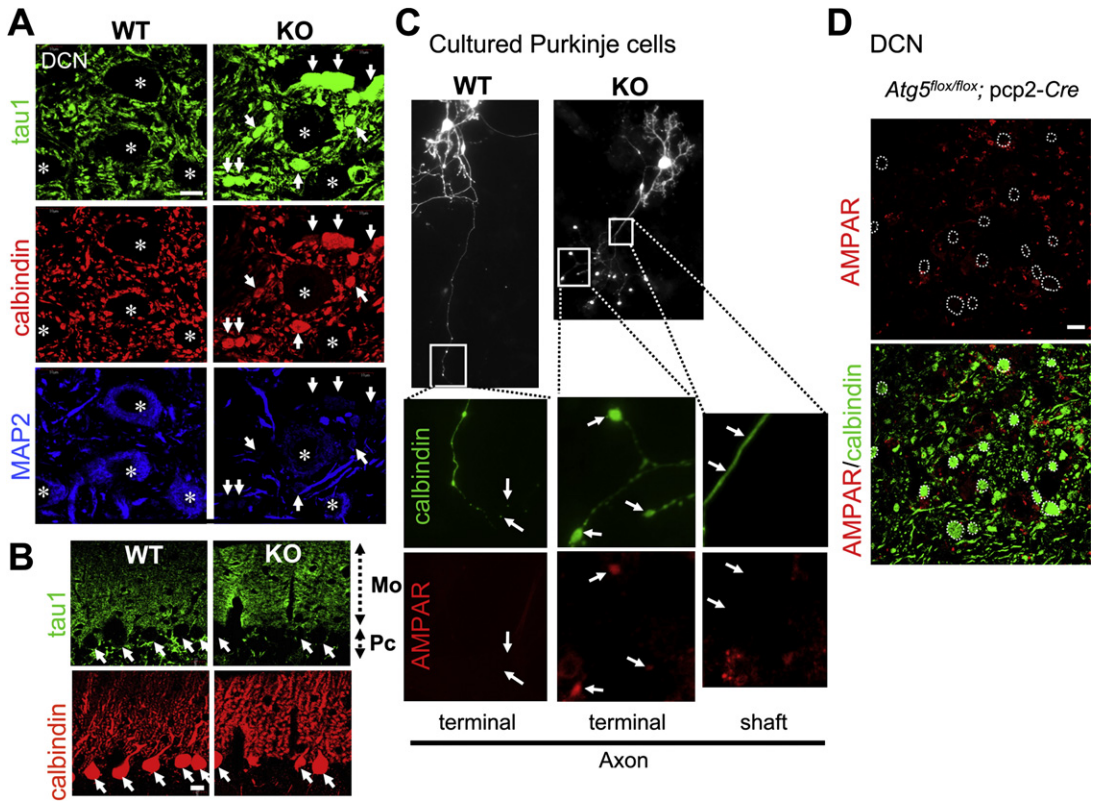

Figure 2. Periterminal Axons Were Swollen in *AP-4β*$^{-/-}$ Purkinje Cells In Vivo and In Vitro

(A) Immunohistochemical analysis of tau1 (green), calbindin (red), and MAP2 (blue) in the DCN region of wild-type (WT) and *AP-4β*$^{-/-}$ (KO) cerebella. The asterisks indicate the soma of DCN neurons, which were positive for MAP2 but negative for tau1 and calbindin, and the arrows indicate calbindin- and tau1-positive axons of Purkinje cells. Scale bar, 10 μm.

(B) Immunohistochemical analysis of tau1 (green) and calbindin (red) in the wild-type and *AP-4β*$^{-/-}$ cerebellar cortices. Calbindin-positive Purkinje cells (Pc) were negative for tau1. Tau1 immunoreactivity in the molecular layer (Mo) corresponded to axons of granule cells that formed synapses on Purkinje-cell dendrites.

(C) Immunocytochemical analysis of endogenous AMPA receptors and calbindin in wild-type (WT) and *AP-4β*$^{-/-}$ (KO) Purkinje cells cultured for 18 days in vitro. An anti-pan-AMPA receptor antibody was used. Axonal regions marked by white squares were enlarged in the lower panels. The arrows and arrowheads indicate the periterminal regions and shafts of Purkinje-cell axons, respectively.

(D) Immunohistochemical analysis of endogenous AMPA receptors (red) and calbindin (green) in the DCN region of *Atg5flox/flox;* pcp2-*Cre* cerebella. Although the calbindin-positive Purkinje-cell axons (dotted lines) were swollen, they were immunonegative for AMPA receptors. Scale bar, 10 μm.

marker in mammals. We found that LC3-II was increased in *AP-4β*$^{-/-}$ cerebellar lysates ($p = 0.042$, $n = 4$; Figure 3C). Furthermore, by breeding transgenic mice that produce green fluorescent protein (GFP)-tagged LC3 (Mizushima et al., 2004) onto an *AP-4β*$^{-/-}$ background (GFP-LC3; *AP-4β*$^{-/-}$), we confirmed that AMPA receptors accumulated in GFP-LC3-labeled autophagosomes in Purkinje cell axons in the DCN region (Figure 3D). Finally, the level of p62/SQSTM1, a protein incorporated into the completed autophagosome and is degraded in the lysosomes (Wang et al., 2006), was decreased in *AP-4β*$^{-/-}$ brain lysates (Figure 3E). Although the source of the aberrant membranous structures remains unclear, these results suggest that AMPA receptors were accumulated in autophagosomes and processed by the autophagic pathway in *AP-4β*$^{-/-}$ axons.

Mislocalized AMPA Receptors within Axons of Hippocampal Neurons

To further investigate the mechanisms underlying mislocalized AMPA receptors in axons, we used cultured hippocampal neurons, in which exogenously expressed membrane proteins have been shown to follow the endogenous sorting rules (Jareb and Banker, 1998). In these experiments, coexpressed GFP was distributed throughout the neurites, making the axons easy to identify by their typical morphology (Silverman et al., 2005); in some experiments, we further confirmed the axonal structures by immunostaining with the dendrite-specific marker MAP2 or the axon marker unphosphorylated tau1.

First, we confirmed that immunoreactivity for endogenous GluR1 was significantly higher in axons of *AP-4β*$^{-/-}$ hippocampal neurons than those in wild-type neurons cultured for 18 days in vitro (DIV) (Figures 4A and 4B). On the other hand, endogenous GluR1 was normally expressed in the dendrites and spines of *AP-4β*$^{-/-}$ hippocampal neurons. Similarly, endogenous AMPA receptors (Figure S7) and GluR2 (Figure 6A) were mislocalized in the axons of *AP-4β*$^{-/-}$ hippocampal neurons. Although endogenous AMPA receptor immunoreactivity in axonal shafts was very weak in *AP-4β*$^{-/-}$ Purkinje cells (Figure 2C), it was often detected in axonal shafts of *AP-4β*$^{-/-}$ hippocampal

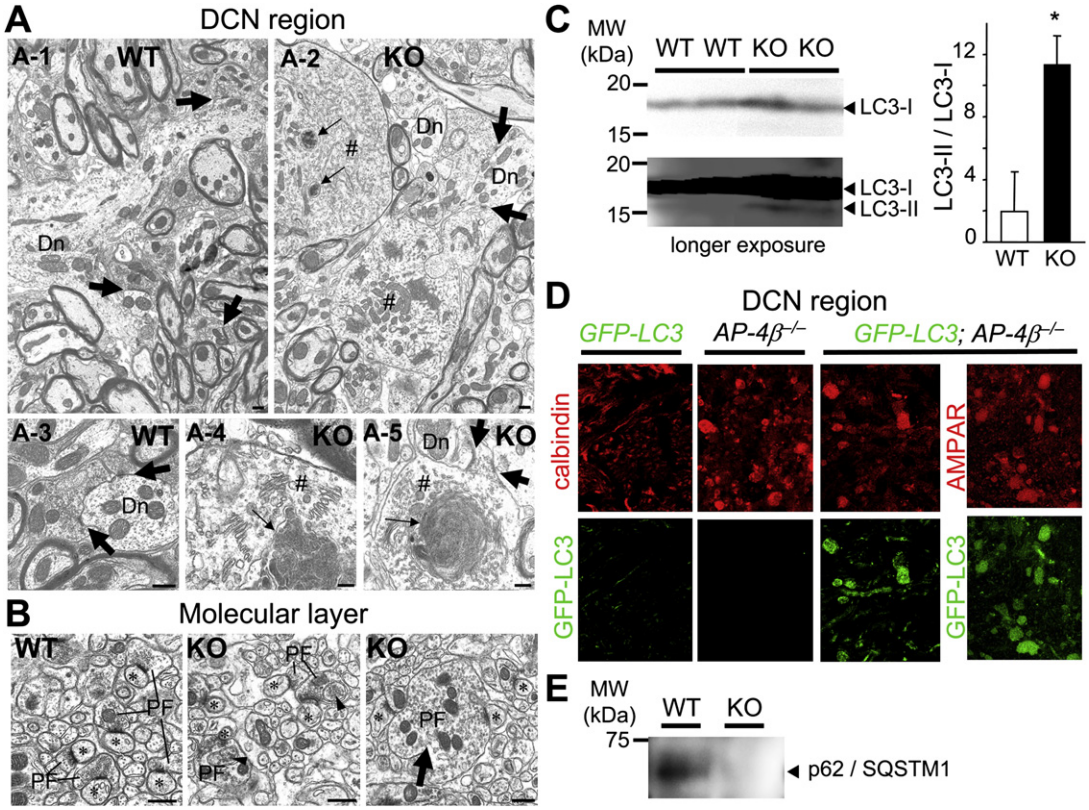

Figure 3. Autophagosome-like Structures within Axons of *AP-4β*$^{-/-}$ Purkinje Cells

(A) Electron microscopic analysis of the DCN regions of wild-type (WT) and *AP-4β*$^{-/-}$ (KO) cerebella. The bold arrows indicate normal synapses, and the thin arrows indicate autophagosome-like and aberrant membranous structures. Dn, dendrites of DCN neurons; #, swollen axons of Purkinje cells. Scale bars, 500 nm.

(B) Electron microscopic analysis of the molecular layers of wild-type (WT) and *AP-4β*$^{-/-}$ (KO) cerebella. PF, parallel-fiber terminals. The asterisks indicate the dendritic spines of Purkinje cells. The arrowheads indicate aberrant parallel fiber terminals containing double-membraned structures. The arrow indicates a swollen parallel fiber terminal. Scale bars, 500 nm.

(C) Activation of the autophagic pathway revealed by immunoblot analysis of LC3-II. Representative immunoblot data using two samples each from wild-type and *AP-4β*$^{-/-}$ mice. The right graph shows a quantitative analysis of the amount of LC3-II protein normalized by that of LC3-I. *p = 0.042; n = 4.

(D) Immunohistochemical analysis of calbindin (red) and GFP-LC3 (green) in the DCN region of GFP-LC3 transgenic mice, *AP-4β*$^{-/-}$ mice, and GFP-LC3 transgenic mice on a background of *AP-4β*$^{-/-}$ mice (*GFP-LC3; AP-4β*$^{-/-}$). Calbindin-positive Purkinje-cell axons were immunopositive for AMPA receptors and GFP-LC3 in the DCN region of *GFP-LC3; AP-4β*$^{-/-}$ cerebella.

(E) Immunoblot analysis of whole brain lysates from wild-type (WT) and *AP-4β*$^{-/-}$ (KO) mice using anti-p62/SQSTM1 antibody. The p62/SQSTM1 level was reduced in the brain of *AP-4β*$^{-/-}$ mice, a result indicating an increased autophagosome-lysosomal degradation activity.

neurons (Figures 4A and 6A); this difference may reflect lower activities of protein degradation pathways (Hara et al., 2006) or the presence of en passant synapses in hippocampal neurons. Unlike in Purkinje cells, changes in the distribution of AMPA receptors were difficult to demonstrate unequivocally in hippocampal neurons in vivo, mainly because the axonal fields of these neurons were often not well separated from their dendritic fields; AMPA receptor immunoreactivity in axons was easily masked by that in dendrites (Mitsui et al., 2005). In addition, the swelling of axons that form en passant synapses may be difficult to detect in vivo. However, by using the Sindbis virus to express the hemagglutinin (HA)-tagged GluR1 subunit of the AMPA receptor in the hippocampus in vivo, we found that the GluR1 subunits were mislocalized in the axons of *AP-4β*$^{-/-}$ hippocampal neurons, but not in wild-type neurons, in vivo (Figure S8). These findings are consistent with the view that AP-4 is required for somatodendritic region-specific localization of AMPA receptors in hippocampal neurons as well as in Purkinje neurons.

Next, we used the Sindbis virus to express GluR1 with its C-terminal region tagged with HA in cultured hippocampal neurons at 17 DIV. One day later, HA immunoreactivity was not observed in GFP-positive and MAP2-negative axons of wild-type hippocampal neurons under permeabilizing conditions. In contrast, HA immunoreactivity was present in the axons of *AP-4β*$^{-/-}$ neurons (Figure 4C). To quantify the portion of HA-tagged GluR1 that was mislocalized in the axons of *AP-4β*$^{-/-}$ hippocampal neurons, we determined the axon-dendrite ratio (ADR) (Rivera et al., 2003); the ratio of HA signals in the axon to those in the dendrites was normalized by the corresponding ratio of GFP signals. Thus, the ADR value of unity indicates that the target protein was nonselectively distributed to both the axonal and dendritic domains in a manner similar to that of the cytosolic protein GFP. The ADR value for HA-GluR1 (0.16 ± 0.14, n = 8) in

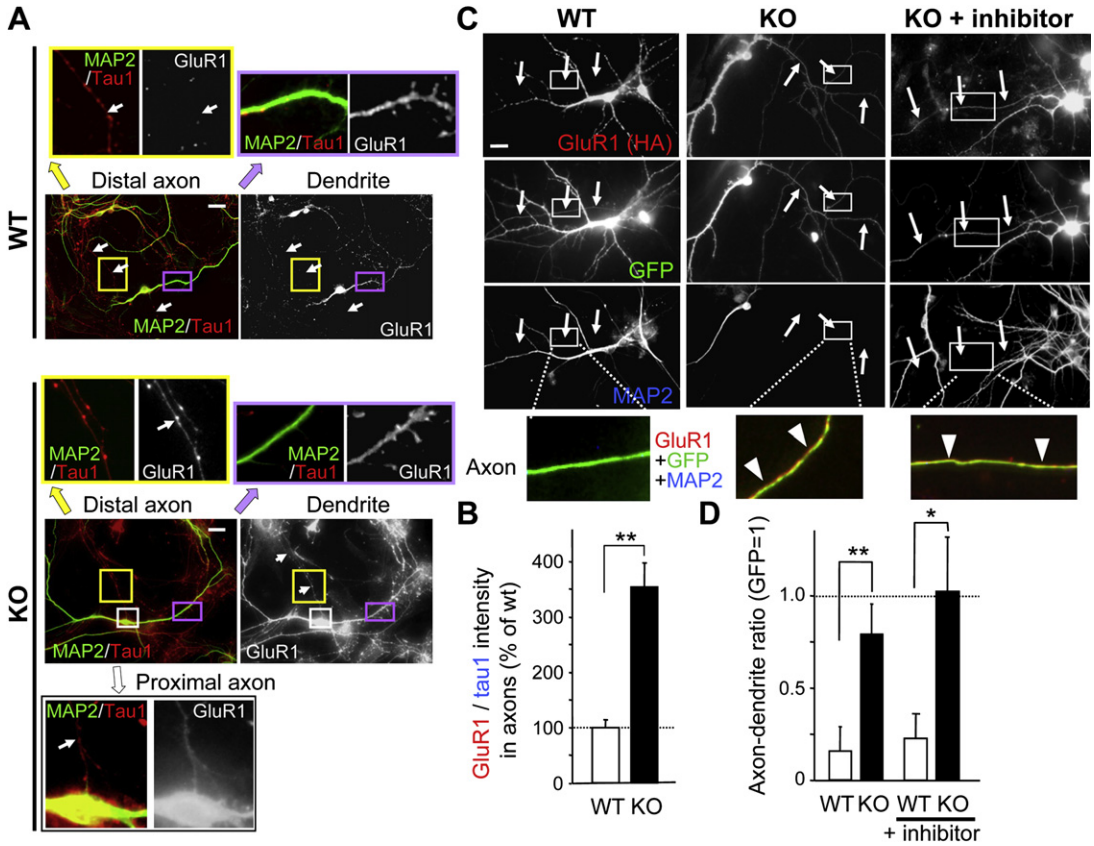

Figure 4. Endogenous and Exogenous AMPA Receptors Were Excluded from Axons of Wild-Type, but Not *AP-4β*$^{-/-}$, Hippocampal Neurons In Vitro

(A) Immunocytochemical analysis of endogenous GluR1 localization using anti-GluR1 antibody in cultured wild-type (WT) and *AP-4β*$^{-/-}$ (KO) hippocampal neurons at 18 DIV. MAP2 (green) and unphosphorylated tau1 (red) immunoreactivities were used to identify the axons. The regions marked by yellow squares (distal axons), white squares (proximal axons), and purple squares (dendrites) are enlarged in the corresponding panels. The arrows indicate the axons. Scale bars, 20 μm.

(B) Quantitative analysis of the fluorescence intensity of axonal GluR1 normalized by the tau1 intensity. The mean value in wild-type neurons was defined as 100%. The axonal fluorescence intensity of anti-GluR1 antibodies was significantly higher in *AP-4β*$^{-/-}$ than in wild-type hippocampal neurons (**p = 0.0023; n = 7).

(C) Immunocytochemical analysis of HA-tagged GluR1 localization in wild-type (WT; left) and *AP-4β*$^{-/-}$ hippocampal neurons without (KO; middle) or with (KO + inhibitor; right) lysosomal inhibitors. HA-tagged GluR1 and GFP were coexpressed in cultured hippocampal neurons using the Sindbis virus at 17 DIV and were immunostained at 18 DIV. The arrows indicate the axons. The regions marked by squares are enlarged in the lower panels. Yellowish axons marked with arrowheads indicate axons expressing GluR1 (red) and GFP (green), but not MAP2 (blue). Scale bar, 20 μm.

(D) Quantitative analysis of the polarized distribution of GluR1. The axon-dendrite ratio (ADR) value of GFP was established as 1. The ADR value of *AP-4β*$^{-/-}$ hippocampal neurons approached unity after treatment with lysosomal inhibitors (+inhibitor). The ADR values were significantly higher in *AP-4β*$^{-/-}$ than in wild-type hippocampal neurons with or without lysosomal inhibitors (*p = 0.036; **p = 0.006; n = 8).

wild-type hippocampal neurons (Figure 4D) was similar to the reported value for the Kv4.2 K channel (0.1 ± 0.02), which is preferentially sorted to the somatodendritic domain via an unknown mechanism (Rivera et al., 2003). The ADR value for HA-GluR1 was significantly higher in *AP-4β*$^{-/-}$ hippocampal neurons (0.80 ± 0.16, n = 8) than in wild-type hippocampal neurons (p = 0.006; Figure 4D). However, since the ADR value for HA-GluR1 was still less than unity, some other mechanism might contribute to the polarized distribution of GluR1 to *AP-4β*$^{-/-}$ axons. Alternatively, the degradation of mislocalized AMPA receptors via the autophagic pathway in axons (Figure 3) may have decreased the ADR value. Indeed, the treatment of *AP-4β*$^{-/-}$ hippocampal neurons with lysosomal inhibitors for 1 day caused the ADR value for HA-GluR1 to approach unity (1.03 ± 0.29, n = 8; Figures 4C and 4D). These results indicate that the somatodendritic distribution of endogenous AMPA receptors can be recapitulated by exogenously expressed AMPA receptors in cultured hippocampal neurons.

Finally, to obtain clues how AMPA receptors are trafficked in axons, we examined the location of AMPA receptors in axons of cultured GFP-LC3; *AP-4β*$^{-/-}$ hippocampal neurons. As observed in Purkinje cell axons in the DCN region in vivo (Figure 3D), endogenous AMPA receptor immunoreactivity and GFP-LC3 accumulated in several regions along the axons of GFP-LC3; *AP-4β*$^{-/-}$ hippocampal neurons in culture (Figure 5A). We also expressed GluR1 with its N-terminal extracellular region tagged

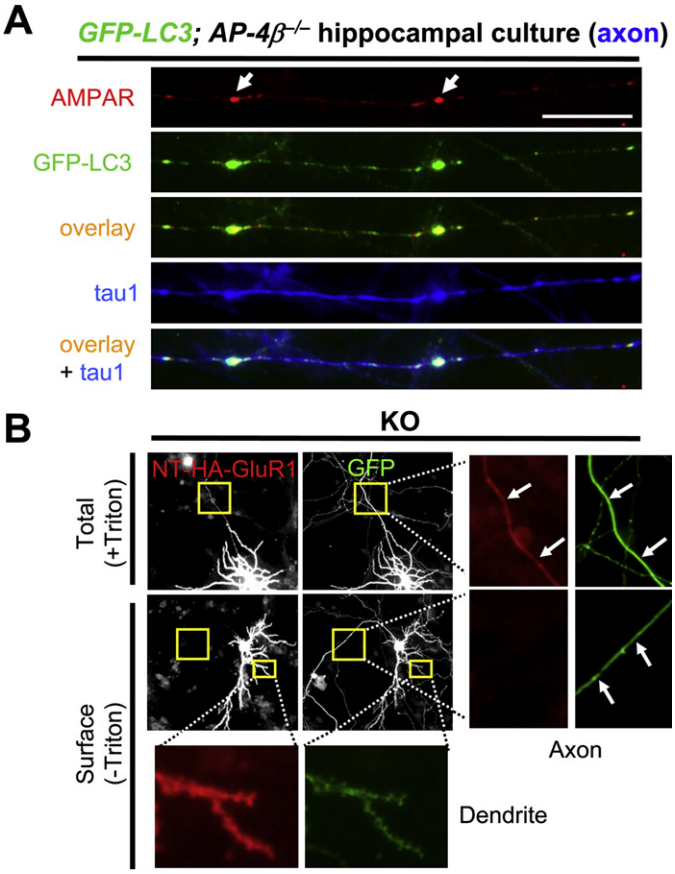

Figure 5. AMPA Receptors Were Accumulated in Axonal Autophagosomes and Do Not Reach Cell Surface in *AP-4β*$^{-/-}$ Hippocampal Neurons

(A) AMPA receptors were mislocalized and accumulated in autophagosomes in the axons of *AP-4β*$^{-/-}$ hippocampal neurons in vitro. Hippocampal neurons prepared from GFP-LC3 transgenic mice on a background of *AP-4β*$^{-/-}$ mice (*GFP-LC3; AP-4β*$^{-/-}$) were fixed and immunostained using an anti-pan-AMPA receptor antibody and an anti-tau1 antibody at 18 DIV. Endogenous AMPA receptors accumulated in LC3-positive autophagosomes (arrows) in the tau1-positive axons. Scale bar, 20 μm.

(B) GluR1 with its N terminus tagged with HA (NT-HA-GluR1) was mislocalized and did not reach the cell surface of axons of *AP-4β*$^{-/-}$ hippocampal neurons. *AP-4β*$^{-/-}$ hippocampal neurons were transfected with NT-HA-GluR1 and GFP at 2 DIV and immunostained using anti-HA antibodies under nonpermeabilizing (– Triton; Surface) and permeabilizing (+ Triton; Total) conditions at 18 DIV. The regions marked by squares were enlarged in the corresponding panels. Although NT-HA-GluR1 was present on the surface of dendrites, it was visible in axons (arrows) only under permeabilizing conditions, a result indicating localization of missorted GluR1 in intracellular components.

with HA (NT-HA-GluR1) in *AP-4β*$^{-/-}$ hippocampal neurons. NT-HA-GluR1 was missorted to the axons of *AP-4β*$^{-/-}$ hippocampal neurons in a manner similar to that of C-terminal HA-GluR1 (Figure S9). An immunocytochemical analysis of NT-HA-GluR1 under nonpermeabilizing conditions revealed that HA-GluR1 was mainly retained intracellularly in the axonal domain, whereas it was abundantly expressed on the surface of dendritic shafts and spines of *AP-4β*$^{-/-}$ hippocampal neurons (Figure 5B). These findings suggest that PDZ proteins that interact with the extreme C termini of AMPA receptors unlikely contributed to the selective distribution of AMPA receptors in the somatodendritic domain and that mislocalized AMPA receptors in axons are accumulated in autophagosomes without reaching the cell surface.

Sorting of Other Membrane Proteins in *AP-4β*$^{-/-}$ Hippocampal Neurons

Polarized membrane protein sorting in neurons is accomplished along the endocytic pathway, the biosynthetic secretory pathway, or a combination of both pathways. For example, axonal membrane proteins, like Nav1.2 Na channel and VAMP2, are selectively endocytosed from the somatodendritic domain after nonselective transport to all domains (Garrido et al., 2001; Sampo et al., 2003), whereas the odorant receptor ODR-10 (Dwyer et al., 2001) and Kv4.2 K channel (Rivera et al., 2003) are directly sorted to the somatodendritic domain via the biosynthetic pathway. Membrane proteins sorted via the endocytic pathway generally lose their polarity when their immunoreactivities are studied under permeabilizing conditions (Garrido et al., 2001; Sampo et al., 2003). Indeed, VAMP2 immunoreactivity was observed in both the dendrites and axons of wild-type hippocampal neurons under permeabilizing conditions, whereas it was selectively localized in the axons under nonpermeabilizing conditions (Figure S10A). Similar results were obtained in *AP-4β*$^{-/-}$ hippocampal neurons (Figure S10B), indicating that the polarized axonal sorting of VAMP2 was intact in these cells. In contrast, endogenous AMPA receptors were not observed in the axons of wild-type Purkinje cells (Figure 2C) or hippocampal neurons (Figure 4A), even under permeabilizing conditions. Furthermore, the coexpression of dominant-negative dynamin 1, which blocks clathrin-mediated endocytosis (Herskovits et al., 1993; Matsuda et al., 2006), had no effect on the somatodendritic distribution of GluR1 immunoreactivity (Figure S11). These results indicate that selective distribution of AMPA receptors in the somatodendritic domain is achieved through the biosynthetic secretory sorting pathway in wild-type neurons.

Interestingly, the immunoreactivities of the NR1 subunit of NMDA receptors (Figure 6B) and mGluR1α (Figure 6C) were selectively targeted to the somatodendritic domain of *AP-4β*$^{-/-}$ hippocampal neurons in vitro. Similarly, GluR1 immunoreactivity (Figure S4A), but not mGluR1α immunoreactivity (Figure S4B), accumulated in calbindin-positive Purkinje cell axons in the DCN region of *AP-4β*$^{-/-}$ cerebella in vivo. Furthermore, GluR2, but not NR1 or mGluR1α, was specifically coimmunoprecipitated with AP-4ε from wild-type, but not from *AP-4β*$^{-/-}$, cerebellar lysates (Figures 6D and 6E). Similarly, AP-4ε and AP-4β were selectively coimmunoprecipitated with GluR2, but not with NR1 or mGluR1α (Figures 6D and 6E). Like NR1 and mGluR1α, transferrin receptor (TfR), which is sorted to the basolateral domain in epithelial cells (Simmen et al., 2002), was normally distributed to the somatodendritic domain of *AP-4β*$^{-/-}$ Purkinje cells (Figure S12A). In contrast, another basolateral protein LDLR was mislocalized in the axonal domain (Figure S12B). Similarly, the δ2 subtype of glutamate receptors, which was shown to bind

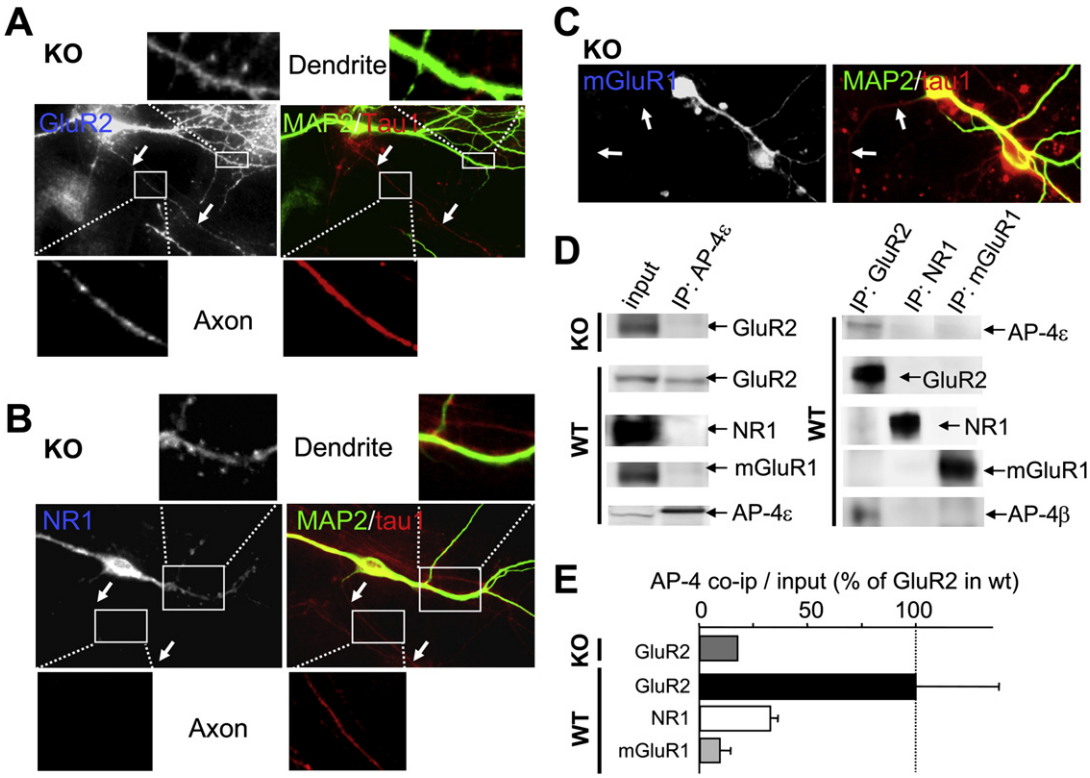

Figure 6. Exclusion of Endogenous GluR2, but Not NR1 nor mGluR1, from Axons Was Dependent on AP-4

(A) Immunocytochemical analysis of endogenous GluR2 localization using anti-GluR2 antibody in cultured *AP-4β*$^{-/-}$ (KO) hippocampal neurons (DIV18). MAP2 (green) and unphosphorylated tau1 (blue) immunoreactivities were used to identify the axons. The regions marked by the squares are enlarged in the corresponding panels. Endogenous GluR2 was mislocalized in the tau1-positive and MAP2-negative axons (arrows), whereas it was normally expressed in the dendrites.

(B) Immunocytochemical analysis of endogenous NR1 localization using anti-NR1 antibody in cultured *AP-4β*$^{-/-}$ (KO) hippocampal neurons (DIV18). MAP2 (green) and unphosphorylated tau1 (blue) immunoreactivities were used to identify the axons. The regions marked by the squares are enlarged in the corresponding panels. Endogenous NR1 was normally excluded from the tau1-positive and MAP2-negative axons (arrows).

(C) Immunocytochemical analysis of endogenous mGluR1 in cultured *AP-4β*$^{-/-}$ hippocampal neurons (DIV18). Endogenous mGluR1 was normally excluded from the tau1-positive and MAP2-negative axons (arrows).

(D) Coimmunoprecipitation assay of interaction between GluR2 and AP-4 in vivo. Cerebellar lysates of *AP-4β*$^{-/-}$ and wild-type mice were immunoprecipitated with anti-AP-4ε antibody (left panels). Proteins in lysates (input) and those coimmunoprecipitated with AP-4ε (IP) were immunoblotted with the indicated antibodies. Similarly, wild-type cerebellar lysates coimmunoprecipitated with anti-GluR2, anti-NR1, or anti-mGluR1 antibody were immunoblotted with anti-AP-4ε, anti-GluR2, anti-NR1, anti-mGluR1, and anti-AP-4β antibodies (right panels).

(E) Quantitative analysis of the coimmunoprecipitation assay. The mean band intensity of AP-4ε that coimmunoprecipitated with GluR2 was established as 100% (n = 3).

to AP-4 (Yap et al., 2003), accumulated in the calbindin-positive Purkinje-cell axons in the DCN region of *AP-4β*$^{-/-}$ cerebella (Figure S12C). These results indicate that AP-4 recognizes specific cargo proteins, such as AMPA receptors, LDLR, and δ2 glutamate receptors, and regulates their selective distribution in the somatodendritic domain of neurons.

To further confirm that the mislocalization of the AMPA receptors was directly caused by the loss of the AP-4 complex, we reintroduced Flag-tagged AP-4β into *AP-4β*$^{-/-}$ hippocampal neurons (Figure S13A). We found that *AP-4β*$^{-/-}$ neurons that expressed Flag-AP-4β also became immunopositive for AP-4ε proteins (Figure S13B), a finding indicating that the loss of AP-4ε protein in *AP-4β*$^{-/-}$ brain (Figure 1B) was indeed caused by the loss of AP-4β protein. Immunocytochemical analyses revealed that HA-tagged GluR1 was mostly excluded from the axons of *AP-4β*$^{-/-}$ neurons that expressed exogenous AP-4β (Figures S13A and S13C). These results indicate that the mislocalization of AMPA receptors in *AP-4β*$^{-/-}$ neurons was caused by the loss of functional AP-4 complex. Furthermore, the selective knockdown of the μ4 subunit of AP-4 by antisense RNA also resulted in the mislocalization of AMPA receptors in axons of wild-type hippocampal neurons (Figures S14–S16). Altogether, these findings are consistent with the view that the loss of *AP-4β* did not cause nonspecific detrimental effects but abrogated trafficking of specific cargo proteins including AMPA receptors in neurons.

TARPs Bind to AP-4 and Regulate the AMPA Receptor Trafficking

The μ subclass of AP complexes is generally responsible for recognizing cargo proteins (Boehm and Bonifacino, 2001). Thus, to examine whether the AMPA receptor was recognized by the μ4

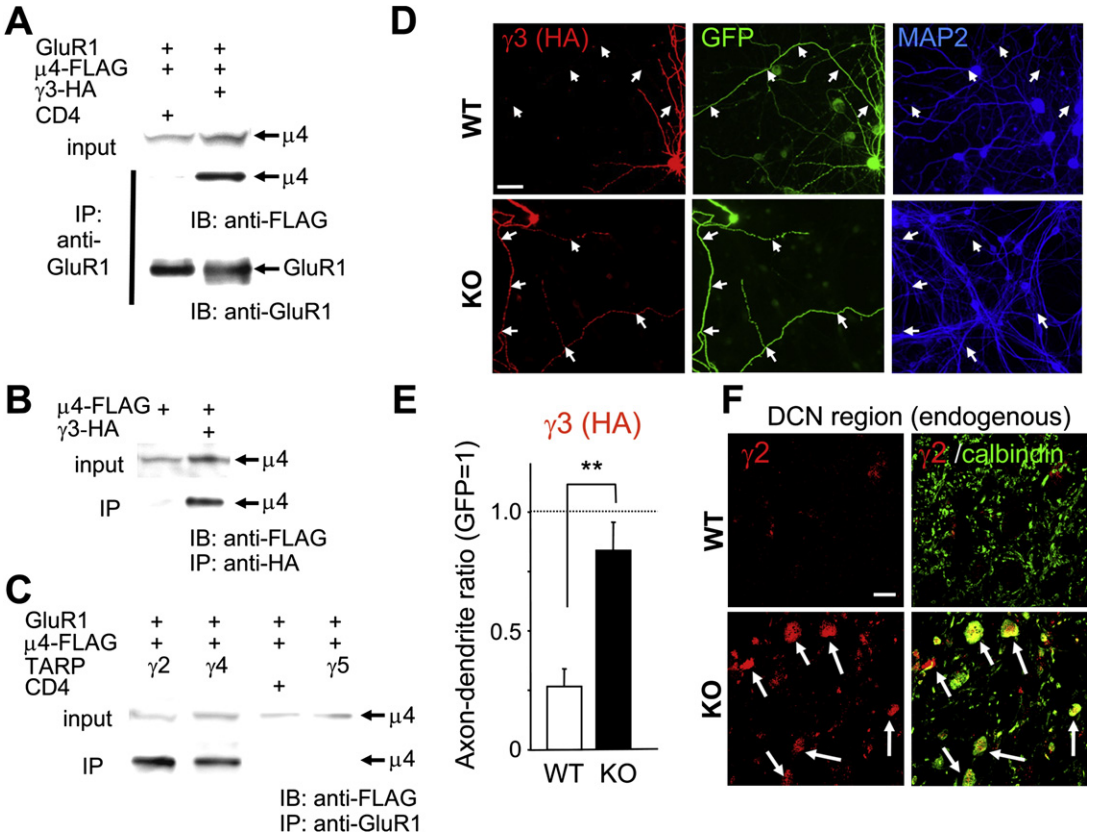

Figure 7. AP-4 Indirectly Binds to GluR1 via TARPs and Controls Distribution of TARPs

(A) Coimmunoprecipitation analysis of interaction between GluR1 and AP-4 μ4. Lysates of HEK293 cells expressing GluR1 and Flag-tagged μ4 were immunoprecipitated (IP) using anti-GluR1 antibody and analyzed using anti-Flag and anti-GluR1 antibodies (IB). Coexpression of TARP γ-3, but not CD4, was necessary for the coimmunoprecipitation of GluR1 and μ4.

(B) Coimmunoprecipitation analysis of the interaction between γ3 and AP-4 μ4. Lysates of HEK293 cells expressing HA-tagged γ3 and Flag-tagged μ4 were immunoprecipitated (IP) using anti-HA antibody and analyzed using anti-Flag antibody (IB).

(C) Requirement of coexpressed TARP family proteins in the interaction between GluR1 and AP-4 μ4 revealed by coimmunoprecipitation analysis. Lysates of HEK293 expressing the indicated combinations of proteins were immunoprecipitated using anti-GluR1 antibody and analyzed using anti-Flag antibody.

(D) Localization of HA-tagged γ3 in wild-type (WT; upper) and *AP-4β*$^{-/-}$ (KO; lower) hippocampal neurons. HA-tagged γ3 and GFP were coexpressed by the Sindbis virus at 17 DIV and analyzed at 18 DIV. HA-tagged γ3 was missorted to MAP2-negative axons (arrows) in *AP-4β*$^{-/-}$, but not in wild-type, hippocampal neurons. Scale bar, 20 μm.

(E) Quantitative analysis of polarized distribution of γ3. The axon-dendrite ratio value of GFP was established as 1. The axonal transport of HA-tagged γ3 was significantly higher in *AP-4β*$^{-/-}$ than in wild-type hippocampal neurons (**p = 0.0023; n = 8).

(F) Immunohistochemical analysis of γ2 (red) and calbindin (green) localization in the DCN region of wild-type (WT) and *AP-4β*$^{-/-}$ (KO) cerebella. The arrows indicate the axons of Purkinje cells, which are doubly immunopositive for calbindin and γ2. Bar represents 10 μm.

subunit of AP-4, we expressed Flag-tagged μ4 and GluR1 in HEK293 cells and performed a coimmunoprecipitation assay. Under our experimental conditions, however, μ4 was not effectively coimmunoprecipitated with GluR1 (Figure 7A) or GluR2 (Figure S17). Recently, TARP family proteins γ2, γ3, γ4, and γ8 have been shown to tightly associate with all subunits of AMPA receptors in vivo (Chen et al., 2000; Tomita et al., 2005b; Vandenberghe et al., 2005). Thus, to explore the possibility that TARPs might be required for AMPA receptors to associate with μ4, we coexpressed GluR1 or GluR2 and Flag-tagged μ4 together with HA-tagged γ3 in HEK293 cells. The μ4 subunit was effectively coimmunoprecipitated with GluR1 (Figure 7A) and GluR2 (Figure S17) when it was coexpressed with γ3, but not when it was coexpressed with an unrelated membrane protein CD4 (Gu et al., 2003). Indeed, μ4 was coimmunoprecipitated by γ3 in the absence of GluR1 (Figure 7B). Similarly, μ4 was coimmunoprecipitated with GluR1 when it was coexpressed with other TARP family proteins, such as γ2 and γ4, but not with γ5 (Figure 7C), which is structurally similar to TARPs but does not modulate AMPA receptor functions (Tomita et al., 2003, 2004). When HA-tagged γ3 was expressed in hippocampal neurons, it was excluded from MAP2-negative axons in wild-type neurons, whereas HA-tagged γ3 was missorted to the axons in *AP-4β*$^{-/-}$ hippocampal neurons (Figure 7D). Similarly, HA-tagged γ2 and γ4 were mislocalized in the axons of *AP-4β*$^{-/-}$ neurons (Figures S18A and S18B). The ADR value for HA-γ3 was significantly higher in *AP-4β*$^{-/-}$ neurons than in wild-type neurons (p = 0.0023, n = 8; Figure 7E). We also found that

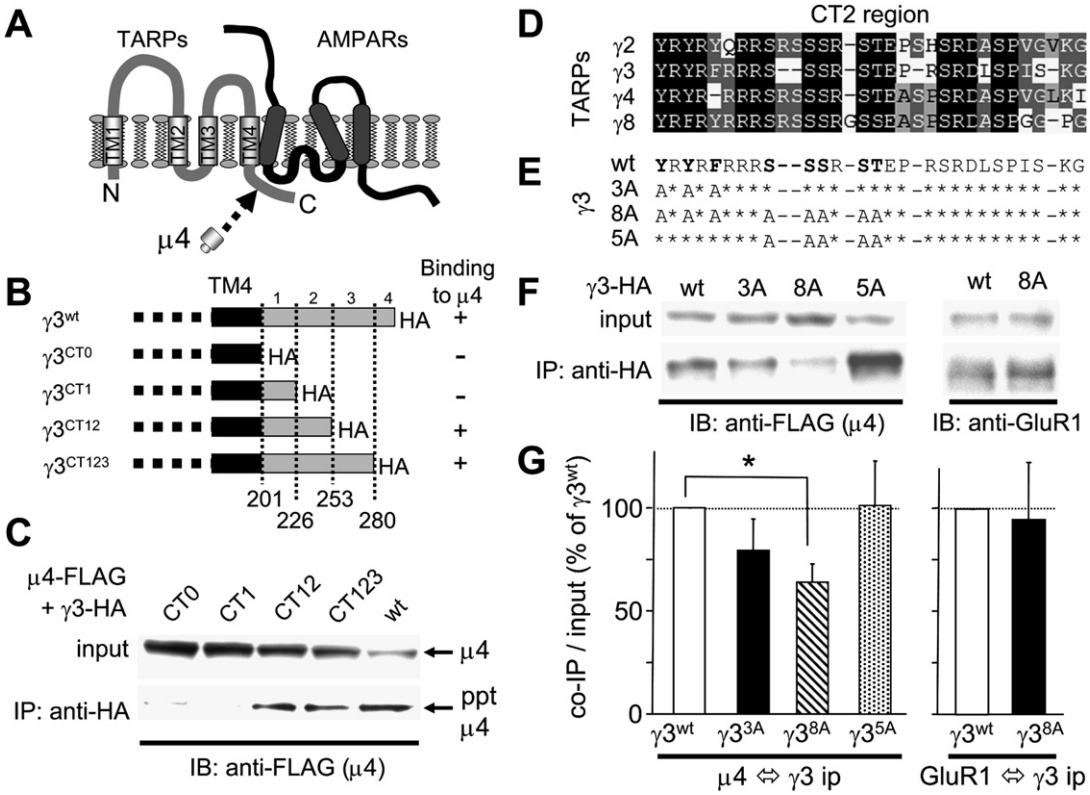

Figure 8. Characterization of the μ4-Binding Domain of TARP γ3

(A) Schematic drawing of the TARP membrane topology. The upper side is the extracellular region, and the lower side is the intracellular region. The C-terminal domain following the fourth transmembrane domain (TM4) covers most of the intracellular regions.

(B) Schematic drawings of the deletion mutants of γ3. The black boxes indicate TM4. Various deletions were introduced to the C-terminal cytoplasmic domain. The lower numbers indicate the amino acid positions.

(C) Interaction between AP-4 μ4 and TARP γ3 mutants. HA-tagged wild-type or mutant γ3 and Flag-tagged μ4 were coexpressed in HEK293 cells, and the cell lysates were subjected to immunoprecipitation with anti-HA antibody and analyzed using an immunoblot analysis with anti-Flag antibody.

(D) Amino acid sequence alignment of TARPs' CT2 regions. The CLUSTALW program of the Biology Workbench Suites (the Computational Biology Group, the National Center for Supercomputing Applications, University of Illinois, Urbana-Champaign, IL) was used. The letters are shaded according to the percentage of conserved similar amino acids (100%, 80%, and 60%) at each position.

(E) List of mutations introduced in the CT2 region of TARP γ3. The first amino acid sequence shows the CT2 region of γ3. The second, third, and fourth amino acid sequences show the mutations that were studied. The asterisk indicates identical amino acids.

(F) Immunoprecipitation assay examining μ4 binding (left panel) or GluR1 binding (right panel) to wild-type and mutant TARP γ3 constructs.

(G) Quantitative analysis of immunoprecipitation assay. The amount of μ4 (left graph) or GluR1 (right graph) that coimmunoprecipitated with wild-type γ3 was arbitrarily established as 100%. *p = 0.045; n = 9.

endogenous γ2 immunoreactivity accumulated in the calbindin-positive Purkinje cell axons in the DCN region of *AP-4β*$^{-/-}$ cerebella (Figure 7F). These results suggest that although it remains unclear whether AP-4 binds directly to TARPs, AP-4 does regulate the polarized distribution of TARPs, which in turn determines the somatodendritic localization of AMPA receptors in neurons.

To further test the hypothesis that TARPs mediate the AP-4-dependent polarized distribution of AMPA receptors in neurons, we next attempted to develop a molecular tool to specifically disrupt the interaction between TARPs and AP-4 in neurons (Figure 8A). Thus, to identify the binding site of γ3 TARP for μ4, we introduced various deletions within the C terminus of γ3 (Figure 8B). HA-tagged wild-type (γ3^{wt}) or mutant (γ3^{CT0}, γ3^{CT1}, γ-3^{CT12}, and γ-3^{CT123}) proteins were coexpressed with Flag-tagged μ4 in HEK293 cells and subjected to a coimmunoprecipitation assay. Although μ4 proteins were coimmunoprecipitated with γ3^{wt}, γ3^{CT123}, and γ3^{CT12}, μ4 was not effectively coimmunoprecipitated with γ3^{CT1} or γ3^{CT0} (Figure 8C). Furthermore, an immunocytochemical analysis using anti-HA antibody and coexpressed GFP in cultured hippocampal neurons revealed that HA-tagged γ3^{CT1}, but not γ3^{wt}, γ3^{CT12}, γ3^{CT123} was mislocalized in axons (Figure S19). These results indicate that the C-terminal region between γ3^{CT1} and γ3^{CT12}, which we will refer to as the CT2 region, is responsible for the binding to μ4 and the polarized sorting of γ3 to the somatodendritic domain in hippocampal neurons.

Because the CT2 region of TARPs is also necessary for its association with AMPA receptors (Tomita et al., 2005a), γ3^{CT1} could not be used as a tool for the specific disruption of interactions between endogenous AMPA receptors and AP-4 in neurons. The μ subunits of all adaptor proteins have been shown to interact preferentially

with a tyrosine-based sorting signal, YXXΦ, in which Φ is a bulky hydrophobic residue (Aguilar et al., 2001). In addition, the binding of μ4 can also be mediated by other tyrosine- or phenylalanine-based signals (Simmen et al., 2002). Because several tyrosine and phenylalanine residues are highly conserved in the CT2 region of all TARPs (Figure 8D), we hypothesized that the binding of μ4 to γ3 might be achieved via a motif based on these residues. We replaced tyrosine and phenylalanine residues in the CT2 region of γ3 with alanine residues ($\gamma3^{3A}$; Figure 8E) and performed a coimmunoprecipitation assay (Figure 8F and 8G). Although the interaction between μ4 and $\gamma3^{3A}$ was reduced from that between μ4 and $\gamma3^{wt}$, the difference was not statistically significant ($p = 0.21$, $n = 8$). Interestingly, these residues are immediately followed by multiple serine and threonine residues (Figure 8E), which have been shown to be phosphorylated in heterologous cells (Tomita et al., 2005b). To examine the possibility that the phosphorylation of serine or threonine residues in the CT2 region of TARP may affect the binding affinity of AP-4 to TARPs, we additionally replaced five subsequent serine and threonine residues with alanine ($\gamma3^{8A}$; Figure 8E). As a result, the interaction with μ4 was significantly reduced (Figure 8F and 8G; $p = 0.045$, $n = 9$). The differences in binding affinity for μ4 were also estimated by an overlay assay using purified C terminus of $\gamma3^{wt}$ or $\gamma3^{8A}$; the amount of HA-tagged μ4 proteins bound to the C terminus of $\gamma3^{8A}$ was approximately one-quarter of that bound to the C terminus of $\gamma3^{wt}$ (Figure S20). In contrast, the amount of μ4 coimmunoprecipitated by $\gamma3^{5A}$, in which five serine and threonine residues were replaced with alanine without replacing the tyrosine and phenylalanine residues (Figure 8E), was similar to that achieved by $\gamma3^{wt}$ (Figures 8F and 8G). The tyrosine and/or phenylalanine motif in the CT2 region of γ3 is probably the main mediator of the binding of γ3 to μ4; the subsequent serine and threonine residues may not be directly involved in the binding to μ4 but may provide a permissive environment. In contrast, because the phosphorylation of the serine or threonine residues in the CT2 region of TARPs does not affect its binding affinity to AMPA receptors (Tomita et al., 2005b), $\gamma3^{8A}$ interacted with AMPA receptors in a manner similar to $\gamma3^{wt}$ (Figures 8F and 8G). These results indicate that the overexpression of $\gamma3^{8A}$ probably specifically blocks the association between endogenous AMPA receptors and AP-4 in a dominant-negative manner.

An immunocytochemical analysis using anti-HA antibody and coexpressed GFP in wild-type hippocampal neurons revealed that HA-tagged $\gamma3^{8A}$ was missorted to MAP2-negative axons (Figures 9A and 9B), a result indicating that $\gamma3^{8A}$ did not significantly bind to endogenous μ4 in hippocampal neurons. As expected from its interaction with AMPA receptors in vitro (Figures 8F and 8G), the expression of $\gamma3^{8A}$, but not of $\gamma3^{wt}$, caused the mislocalization of endogenous AMPA receptors in axons (Figures 9C and 9D and Figure S21). In contrast, AMPA receptors were normally expressed in the dendrite and spines of neurons expressing $\gamma3^{8A}$ (Figure 9C). These results support the hypothesis that endogenous TARPs mediate the polarized distribution of AMPA receptors by interacting with AP-4 in wild-type neurons.

DISCUSSION

In this paper, we demonstrated that the adaptor complex AP-4 plays a unique role in AMPA receptor trafficking in neurons; AMPA receptors were mislocalized and accumulated in autophagosomes in the axons of *AP-4*$\beta^{-/-}$ Purkinje cells and hippocampal neurons both in vivo and in vitro. Although the μ4 subunit of AP-4 did not directly interact with the AMPA receptors, it associated with the AMPA receptor auxiliary subunit TARPs, which then controlled the polarized distribution of AMPA receptors in cultured hippocampal neurons. Our findings have important implications for the general function of adaptor complex AP-4 in neurons and suggest a new role for TARPs in the regulation of AMPA receptor functions. Moreover, our data shed new light on the molecular mechanisms underlying the polarized distribution of certain membrane proteins to the somatodendritic domain in neurons.

AP-4-Dependent AMPA Receptor Trafficking in Neurons

Despite recent progress in our understanding of postsynaptic AMPA receptor trafficking mechanisms, a fundamental question has remained largely unanswered: how is the polarized transport of AMPA receptors to the somatodendritic domain controlled in neurons? In epithelial cells, polarized sorting to the basolateral domain, a functional equivalent of the somatodendritic domain of neurons (Dotti and Simons, 1990; Jareb and Banker, 1998), is achieved by adaptor complexes AP-1B and AP-4 in the TGN or in recycling endosomes (REs) (Folsch et al., 1999; Simmen et al., 2002). Recent works have indicated that AP-1B is mainly localized in REs (Folsch et al., 2003; Gan et al., 2002), whereas AP-4 is mostly associated with the TGN in epithelial cells (Barois and Bakke, 2005; Boehm et al., 2001; Simmen et al., 2002). Thus, certain newly synthesized proteins may transit directly to REs, where they are recognized by AP-1B and sorted to the basolateral membrane (Folsch et al., 2003). For example, newly synthesized TfR appears first in endosomes before reaching the basolateral surface of epithelial cells and sorted mainly by the AP-1B complex at REs (Ang et al., 2004). Alternatively, certain membrane proteins on the cell surface may be endocytosed and transported to REs, where AP-1B-dependent basolateral sorting occurs (Gan et al., 2002). In contrast, certain newly synthesized cargo proteins are thought to be recognized by AP-4 at the TGN and then transported directly to the basolateral membrane (Rodriguez-Boulan and Musch, 2005). Indeed, the selective knockdown of the μ4 subunit of AP-4 by antisense RNA was previously shown to result in the nonselective distribution of several basolateral membrane proteins, such as furin, mannose 6-phosphate receptor, and LDLR, but not TfR, to both the basolateral and apical domains of epithelial cells (Simmen et al., 2002). Similarly, we demonstrated that the disruption of AP-4 resulted in mislocalization of LDLR (Figure S12A), but not TfR (Figure S12B), in axons of *AP-4*$\beta^{-/-}$ Purkinje cells. These findings suggest that AMPA receptor-TARP complexes may be sorted by AP-4 via a biosynthetic pathway in neurons in a manner similar to the AP-4-based sorting that occurs in epithelial cells (Figure S22).

Nevertheless, unlike AP-4-dependent polarized sorting in epithelial cells, mislocalized AMPA receptors accumulated in autophagosomes within the axons and did not reach cell surface (Figures 3 and 5). AMPA receptors may accumulate intracellularly because axonal membranes lack the vesicle fusion apparatus, such as the exocyst complex and the soluble N-ethylmaleimide-sensitive factor complex, which coordinates

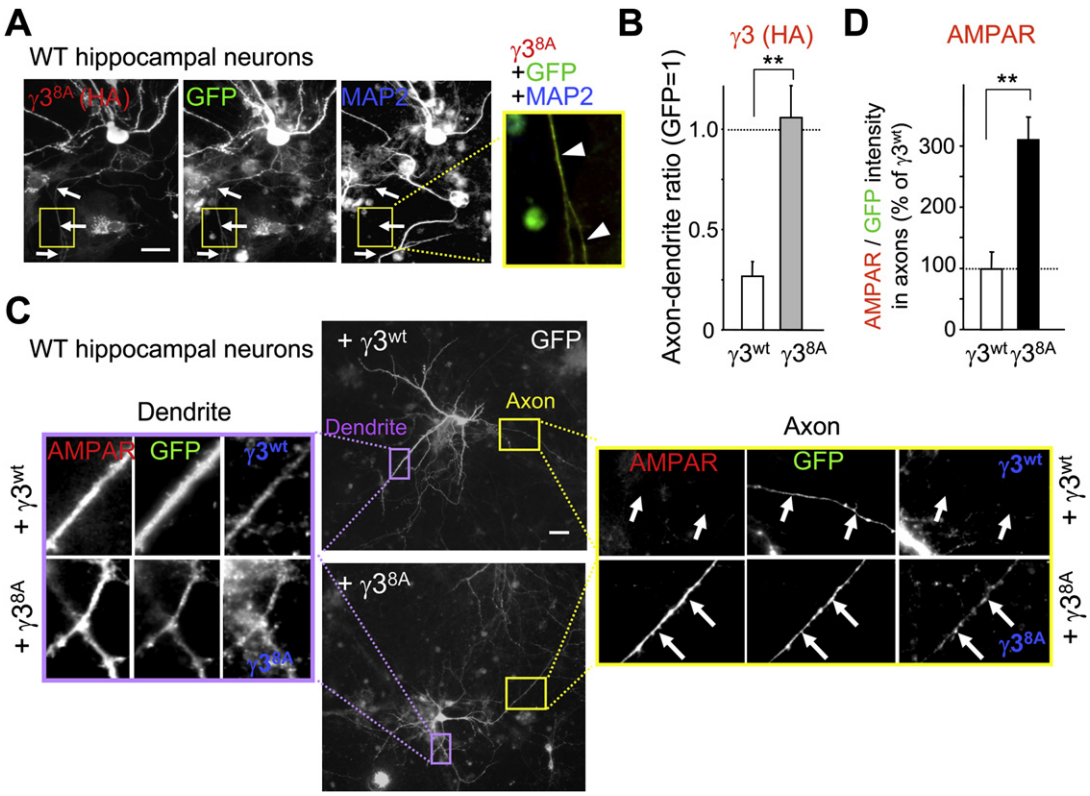

Figure 9. Exclusion of Endogenous AMPA Receptors from Axons Requires the Interaction between Endogenous TARP and AP-4 μ4

(A) Mislocalization of $\gamma3^{8A}$ to the axon of wild-type hippocampal neurons. HA-tagged $\gamma3^{8A}$, which showed a normal association with AMPA receptors but a reduced association with AP-4 μ4 (Figures 8F and 8G), and GFP were coexpressed in wild-type hippocampal neurons at 17 DIV using the Sindbis virus. An immunocytochemical analysis at 18 DIV using anti-MAP2 and anti-HA antibodies revealed that HA-tagged $\gamma3^{8A}$, but not $\gamma3^{wt}$, was mislocalized in the axons (arrows). The regions marked by the squares are enlarged in the right panel. Yellowish axons marked with arrowheads indicate axons expressing $\gamma3^{8A}$ (red) and GFP (green), but not MAP2 (blue).

(B) Quantitative analysis of polarized distribution of γ3. The axon-dendrite ratio value of GFP was defined as 1. The axonal transport of HA-tagged $\gamma3^{8A}$ was significantly higher in *AP-4*$\beta^{-/-}$ than in $\gamma3^{wt}$ (**p = 0.0005; n = 7).

(C) Effects of expression of $\gamma3^{8A}$ on the location of endogenous AMPA receptors in wild-type hippocampal neurons. HA-tagged $\gamma3^{wt}$ or $\gamma3^{8A}$ and GFP were coexpressed in cultured hippocampal neurons using the Sindbis virus at 17 DIV, and an immunocytochemical analysis was performed at 18 DIV using anti-MAP2 and anti-HA antibodies. The regions marked by purple squares (dendrites) or yellow squares (axons) are enlarged in the corresponding panels. The arrows indicate the axons. Although AMPA receptors and γ3 were normally distributed to the dendritic domain, they were mislocalized in the axons of neurons expressing $\gamma3^{8A}$, but not $\gamma3^{wt}$. Scale bar, 20 μm.

(D) Quantitative analysis of the fluorescence intensity of axonal AMPA receptors normalized by the GFP intensity. The value in neurons expressing $\gamma3^{wt}$ was arbitrarily defined as 100%. The axonal transport of endogenous AMPA receptors was significantly increased in hippocampal neurons expressing $\gamma3^{8A}$ (**p = 0.0006; n = 8).

targeted fusion of AMPA receptor-containing vesicles with the plasma membrane (Horton and Ehlers, 2003). Indeed, when expressed in polarized epithelial cells, mislocalized GluR1 could reach cell surface of both basolateral and apical domains (Bedoukian et al., 2008). Alternatively, axons may be equipped with an efficient degradation pathway to eliminate mislocalized proteins. It is also possible that AP-4 may have some direct roles in the regulation of membranes involved in the autophagic pathway. For example, AP-4 interacts with the lysosomal cargo proteins such as LAMP-2 and mediates their direct transport to lysosomes (Aguilar et al., 2001). Further studies are warranted to clarify the role of AP-4 in the formation of autophagosomes containing AMPA receptors in axons.

Cargo Proteins Recognized by AP-4 in Neurons

Although mGluR1 and NR1 subunits of glutamate receptors are also known to be expressed selectively in the somatodendritic domain, their distribution was not affected in *AP-4*$\beta^{-/-}$ Purkinje cells (Figures S4B and S4C) and hippocampal neurons (Figures 6B and 6C). Indeed, unlike AMPA receptors, mGluR1 and NR1 did not coimmunoprecipitate with AP-4 from the brain lysates (Figures 6D and 6E). Similarly, the basolateral or somatodendritic expression of TfR was only marginally affected in μ4-depleted epithelial cells (Simmen et al., 2002) and *AP-4*$\beta^{-/-}$ Purkinje cells. Because neurons lack AP-1B, certain somatodendritic cargos, such as mGluR1, NR1, and TfR, are likely recognized by unknown adaptor proteins other than AP-4 and AP-1B.

Using a combinational peptide approach, the μ4 subunit has been shown to interact with classical tyrosine motifs (Aguilar et al., 2001). However, a surface plasmon resonance assay and a coprecipitation assay revealed the binding of μ4 to phenylalanine- and nonclassical tyrosine-containing motifs: FI in furin, MEQF in MPR, and YSY in LDLR (Simmen et al., 2002). Similarly, we found that an unconventional motif containing phenylalanine and tyrosine (YRYRF; Figure 8E) was essential for the binding of TARP γ3 to μ4; this result indicates that the binding of μ4 to the target protein may be relatively promiscuous and may depend on the cellular context. A motif containing FR and FTF in the C terminus of the δ2 subtype of glutamate receptors was also shown to bind to the μ4 subunit of AP-4 (Yap et al., 2003). Interestingly, motifs containing FR or YR are also highly conserved in odorant receptors, which are selectively sorted to the somatodendritic domain of neurons in *Caenorhabditis elegans* (Dwyer et al., 2001). These motifs are recognized by the μ1 subunit of AP-1 in *C. elegans*; thus, the role of AP-4 might be performed by AP-1, since *C. elegans* lacks AP-4. Furthermore, phenylalanine-containing sequences have been reported to mediate the polarized sorting of several other membrane proteins, like telencephalin (Mitsui et al., 2005) and excitatory amino acid transporter 4 (Cheng et al., 2002). Therefore, in addition to TARP-AMPA receptors, LDLR, and δ2 glutamate receptors, AP-4 may control the polarized sorting of several other membrane proteins in mammalian neurons.

Function of TARPs in AMPA Receptor Trafficking

TARP family proteins, γ2, γ3, γ4, and γ8, are tightly associated with AMPA receptor subunits GluR1–GluR4 and are essential for (1) the cell surface expression of AMPA receptors, (2) the maintenance of synaptic AMPA receptors via association with the anchoring protein PSD-95, and (3) the acceleration of AMPA current kinetics (Chen et al., 2000; Tomita et al., 2005a). In addition to these three functions, we have demonstrated that TARPs associate with the μ4 subunit of AP-4 and mediate polarized sorting of AMPA receptors to the somatodendritic domain. Although no data were shown, a direct interaction between the μ4 subunit and γ3 TARP has also been previously mentioned (Yap et al., 2003). The γ2 subunit of TARP, known as stargazin, promotes the surface expression of AMPA receptors mainly by facilitating the export of AMPA receptors from the ER (Tomita et al., 2003; Vandenberghe et al., 2005). Thus, we postulate that AMPA receptors associate with TARPs at the ER and are exported to the TGN and post-Golgi organelles, where AP-4 binds to the TARPs and possibly to some motor proteins, thereby inducing polarized transport to the somatodendritic domain.

Six μ subunits of the four AP complexes share considerable sequence similarities with each other but localize to different cellular membranes, such as the plasma membrane, the endosome, the TGN, and the lysosome. Similarly, the γ8 and γ2 subunits of TARPs were recently shown to localize to distinct cellular membranes (Inamura et al., 2006). Thus, some TARP family proteins may bind to μ subunits other than μ4, thereby regulating AMPA receptor trafficking between distinct cellular membranes. To understand the regulatory mechanisms underlying AMPA receptor trafficking in neurons, the roles of AP complexes and TARP family proteins need to be clarified further.

Presynaptic AMPA Receptors

Although the majority of AMPA receptors are preferentially transported to the somatodendritic domain, AMPA receptors are also shown to function at the presynaptic axon terminals of certain synapses (Fabian-Fine et al., 2000; Lu et al., 2002; Takago et al., 2005). Such presynaptic AMPA receptors are thought to regulate the motility of axonal filopodia during early development (Chang and De Camilli, 2001; Tashiro et al., 2003) and participate in autocrine or paracrine feedback signals responsible for the modulation of neurotransmitter release (Lee et al., 2002). Because AP-4 and TARP family proteins are expressed ubiquitously throughout the brain, there may be a regulated mechanism by which presynaptic AMPA receptors first escape from the AP-4-based somatodendritic sorting system and then reach the cell surface. For example, the phosphorylation of tyrosine, serine, or threonine residues in the CT2 region of TARP may regulate the binding affinity of AP-4 to TARPs. Similarly, the phosphorylation of a serine residue immediately preceding the YXXΦ signal of aquaporin 4 by casein kinase II enhances interactions with the μ3A subunit of AP-3 and the lysosomal targeting of the protein (Madrid et al., 2001). Indeed, almost all the serine and threonine residues within the CT2 region of γ2 TARP have been shown to be phosphorylated or dephosphorylated in neurons in an activity-dependent manner (Tomita et al., 2005b). We also found that these serine and threonine residues were necessary for the optimal binding of μ4 to γ3 (Figures 8E and 8F). Further study on the regulation of the somatodendritic sorting system based on the TARP-AP-4 complex should provide a better understanding of how functional presynaptic AMPA receptors are transported to the axonal domain under certain physiological conditions.

EXPERIMENTAL PROCEDURES

Knockout and Transgenic Mice

AP-4β$^{-/-}$ mice were generated on a 129T2/Sv background under a contract with Lexicon Genetics (The Woodlands, Texas). They were backcrossed to C57BL/6J mice for seven generations. GFP-LC3 transgenic mice and *Atg5*$^{flox/flox}$ mice were kindly provided by Dr. N. Mizushima (Tokyo Medical and Dental University). To generate Purkinje cell-specific *Atg5*-deficient mice, *Atg5*$^{flox/flox}$ mice were crossed with pcp2-*Cre* transgenic mice (Jackson Laboratory), as described previously (Nishiyama et al., 2007). All procedures related to the care and treatment of the animals were conducted in accordance with Keio University's Guidelines for Animal Experiments.

Microscopic Analysis

Histological assays for the mouse cerebellar slices were performed as previously described (Hirai et al., 2005). Microslicer sections were incubated overnight with the following primary antibodies: rabbit or mouse anti-calbindin (Hirai et al., 2005), guinea pig anti-pan-AMPA receptors, guinea pig anti-GluR2 (Fukaya et al., 2006), guinea pig anti-vesicular GABA transporter (VGAT) (Uchigashima et al., 2007), mouse anti-unphosphorylated tau, rabbit anti-MAP2, rabbit anti-γ2 (Chemicon International), guinea pig anti-mGluR1α (Tanaka et al., 2000). Sections were incubated for 1 hr with Cy3- or FITC-labeled species-specific secondary antibodies. The stained slices were analyzed by confocal microscopy (Olympus). Electron microscopic analysis was performed on parasagittal sections through the cerebellar vermis using an H7100 electron microscope (Hitachi), as reported previously (Hirai et al., 2005).

Dissociated cultures of hippocampal or cerebellar neurons were prepared from embryonic day 17 to 18 mice, as described previously (Matsuda et al., 2006). Hippocampal neurons were transfected using Effectene (QIAGEN) at 2 DIV or infected using the Sindbis virus at 17 DIV (Matsuda et al., 2006). At

18 DIV, the neurons were fixed with 4% paraformaldehyde in phosphate-buffered saline (PBS). For lysosomal inhibition, 10 μg/ml of pepstatin A (Peptide Institute) and 10 μg/ml of E64D (Peptide Institute) were added to the culture medium at 17 DIV. The cultures were first incubated with a blocking solution (1% bovine serum albumin, 0.4% Triton X-100, and 10% normal goat serum in PBS) and were then incubated with the primary antibodies at the following dilutions: rat anti-HA, 1:1,000 (Roche Applied Science); mouse anti-unphosphorylated tau, 1:300 (Chemicon International); rabbit anti-NR1 (Chemicon International); guinea pig anti-GluR1, 1:500; guinea pig anti-GluR2, 1:300; guinea pig anti-pan AMPA receptor, 1:500 (Fukaya et al., 2006); and rabbit anti-MAP2, 1:1,000 (Chemicon International). For visualization, appropriate secondary antibodies conjugated to Alexa 546 or 350 (diluted at 1:1,000; Invitrogen) were used. Cell surface staining of HA-tagged proteins were performed as described in the Supplemental experimental procedures.

Image Quantification

Image analysis was performed in a blind manner without knowledge of the origin of the samples. Fluorescence images were captured using a CCD camera (DP 70, Olympus) attached to a fluorescence microscope (BX60, Olympus) and were analyzed using IP-Lab software (Scanalytics), as described previously (Hirai et al., 2005). Only transfected neurons with well-differentiated dendrites and axons were chosen for the analysis. MAP2 or unphosphorylated tau1 staining was used to differentiate the dendrites from the axons. For the statistical analysis of polarized distribution of AMPA receptors, the intensity of immunoreactivity for HA or endogenous proteins was measured and normalized using the value of coexpressed GFP or that of endogenous tau1 immunoreactivity in the axons. The ADR value was also calculated according to the method described by Rivera et al. (2003) as follows:

$$\mathrm{ADR} = (\mathrm{HA}_{\mathrm{axon}}/\mathrm{HA}_{\mathrm{dendrite}})/(\mathrm{GFP}_{\mathrm{axon}}/\mathrm{GFP}_{\mathrm{dendrite}}),$$

where $\mathrm{HA}_{\mathrm{axon}}$ and $\mathrm{HA}_{\mathrm{dendrite}}$ represent the HA immunoreactivity of HA-tagged GluR1 or TARPs in the axon and dendrite, respectively, and $\mathrm{GFP}_{\mathrm{axon}}$ and $\mathrm{GFP}_{\mathrm{dendrite}}$ represent the fluorescence intensity of GFP in the axon and dendrite, respectively. Since the amount of protein in the somatic region was sometimes very high, the fluorescence intensity was measured between 40 μm and 200 μm from the soma. Segments fasciculate with other neurites or regions were excluded from the measurement.

Immunoprecipitation and Immunoblot Assays

Transfected HEK293 cells or wild-type or *AP-4β*$^{-/-}$ cerebella were solubilized in 500 μl of TNE buffer (50 mM NaCl, 10% NP-40, 20 mM EDTA, 0.1% SDS, 50 mM Tris-HCl [pH 8.0]) supplemented with a protease inhibitor cocktail (Calbiochem). Five microliters of the soluble fraction (the crude fraction) were subjected to immunoblot analysis with anti-AP-4ε antibody (provided by Dr. M. Robinson, Cambridge University, Cambridge, UK), anti-AP-4β antibody, anti-β-actin antibody (Sigma), anti-LC3 antibody (MBL), or anti-p62/SQSTM1 antibody (American Research Products). Anti-AP-4β antibody was produced in the rabbit against C-terminal 39 amino acid residues of the mouse sequence (GenBank BC056200), which was expressed as a glutathione S-transferase (GST) fusion protein using the vector pGEX-4T-2 (GE Healthcare). Fusion proteins were emulsified with Freund's complete or incomplete adjuvant (DIFCO) and injected subcutaneously into female rabbits at intervals of 2 weeks. From antisera, specific antibodies were purified using GST-free polypeptides coupled to Sepharose 4B (Amersham Pharmacia).

For the immunoprecipitation assays, one microgram of anti-HA (Roche), anti-AP-4ε, anti-GluR2 (Matsuda et al., 2000), anti-NR1, or anti-mGluR1 antibody was added to the remaining samples, and the mixture was incubated for 1 hr at 4°C. Then, 50 μl of protein G-conjugated agarose (Amersham Pharmacia) was added, and this mixture was incubated for 1 hr at 4°C. After the precipitates were washed four times with 500 μl of TNE buffer, 50 μl of SDS-PAGE sample buffer was added and the samples were incubated for 5 min at 95°C. After centrifugation, 5 μl of the supernatant was analyzed using immunoblotting with anti-Flag (Sigma) or other various primary antibodies, TrueBlot HRP-conjugated secondary antibody (eBioscience) and the ECL plus kit (Amersham Pharmacia).

Construction and Transfection of Expression Plasmids

Utilizing a PCR method and Pyrobest (Takara), cDNA encoding an HA or Flag tag was added to the 5′ end (immediately following the signal sequence) or 3′ end (immediately upstream of the stop codon) of mouse GluR1, mouse TARP, or mouse μ4 cDNAs. The nucleotide sequences of the amplified open reading frames were confirmed by bidirectional sequencing. The cDNA encoding human CD4 was kindly provided by Dr. D. Vignali (St. Jude Children's Research Hospital). After the cDNAs were cloned into the expression vectors, either pTracer (Invitrogen) or pCAGGS (provided by Dr. J Miyazaki, Osaka University, Osaka, Japan), the constructs were transfected into human embryonic kidney 293 (HEK293) cells using the CellPhect transfection kit (Amersham Pharmacia) or were expressed in hippocampal neurons using Effectene (QIAGEN) or Sindbis virus, as described previously (Matsuda et al., 2006).

Statistical Analysis

The statistical analyses were performed using a Student t test. The results are expressed as the mean ± SEM.

SUPPLEMENTAL DATA

The Supplemental Data for this article can be found online at http://www.neuron.org/cgi/content/full/57/5/730/DC1/.

ACKNOWLEDGMENTS

This work was supported by a grant-in-aid for young scientists (to S.M. and K.M.), Keio Gijuku academic development funds, a Keio University grant-in-aid for the encouragement of young medical scientists (to S.M.), the Naito Memorial Foundation (to K.M.), and a grant-in-aid for scientific research on a priority area (to M.Y.). We thank J. Motohashi, S. Narumi, and N. Kakiya for their technical assistance.

Received: April 9, 2007
Revised: October 8, 2007
Accepted: February 4, 2008
Published: March 12, 2008

REFERENCES

Aguilar, R.C., Boehm, M., Gorshkova, I., Crouch, R.J., Tomita, K., Saito, T., Ohno, H., and Bonifacino, J.S. (2001). Signal-binding specificity of the mu4 subunit of the adaptor protein complex AP-4. J. Biol. Chem. *276*, 13145–13152.

Ang, A.L., Taguchi, T., Francis, S., Folsch, H., Murrells, L.J., Pypaert, M., Warren, G., and Mellman, I. (2004). Recycling endosomes can serve as intermediates during transport from the Golgi to the plasma membrane of MDCK cells. J. Cell Biol. *167*, 531–543.

Barois, N., and Bakke, O. (2005). The adaptor protein AP-4 as a component of the clathrin coat machinery: a morphological study. Biochem. J. *385*, 503–510.

Bedoukian, M.A., Whitesell, J.D., Peterson, E.J., Clay, C.M., and Partin, K.M. (2008). The stargazin C terminus encodes an intrinsic and transferable membrane sorting signal. J. Biol. Chem. *283*, 1597–1600.

Boehm, M., and Bonifacino, J.S. (2001). Adaptins: the final recount. Mol. Biol. Cell *12*, 2907–2920.

Boehm, M., Aguilar, R.C., and Bonifacino, J.S. (2001). Functional and physical interactions of the adaptor protein complex AP-4 with ADP-ribosylation factors (ARFs). EMBO J. *20*, 6265–6276.

Chang, S., and De Camilli, P. (2001). Glutamate regulates actin-based motility in axonal filopodia. Nat. Neurosci. *4*, 787–793.

Chen, L., Chetkovich, D.M., Petralia, R.S., Sweeney, N.T., Kawasaki, Y., Wenthold, R.J., Bredt, D.S., and Nicoll, R.A. (2000). Stargazin regulates synaptic targeting of AMPA receptors by two distinct mechanisms. Nature *408*, 936–943.

Cheng, C., Glover, G., Banker, G., and Amara, S.G. (2002). A novel sorting motif in the glutamate transporter excitatory amino acid transporter 3 directs its targeting in Madin-Darby canine kidney cells and hippocampal neurons. J. Neurosci. *22*, 10643–10652.

Dell'Angelica, E.C., Shotelersuk, V., Aguilar, R.C., Gahl, W.A., and Bonifacino, J.S. (1999). Altered trafficking of lysosomal proteins in Hermansky-Pudlak

syndrome due to mutations in the beta 3A subunit of the AP-3 adaptor. Mol. Cell *3*, 11–21.

Dilaver, G., Schepens, J., van den Maagdenberg, A., Wijers, M., Pepers, B., Fransen, J., and Hendriks, W. (2003). Colocalisation of the protein tyrosine phosphatases PTP-SL and PTPBR7 with beta4-adaptin in neuronal cells. Histochem. Cell Biol. *119*, 1–13.

Dotti, C.G., and Simons, K. (1990). Polarized sorting of viral glycoproteins to the axon and dendrites of hippocampal neurons in culture. Cell *62*, 63–72.

Dwyer, N.D., Adler, C.E., Crump, J.G., L'Etoile, N.D., and Bargmann, C.I. (2001). Polarized dendritic transport and the AP-1 mu1 clathrin adaptor UNC-101 localize odorant receptors to olfactory cilia. Neuron *31*, 277–287.

Fabian-Fine, R., Volknandt, W., Fine, A., and Stewart, M.G. (2000). Age-dependent pre- and postsynaptic distribution of AMPA receptors at synapses in CA3 stratum radiatum of hippocampal slice cultures compared with intact brain. Eur. J. Neurosci. *12*, 3687–3700.

Folsch, H., Ohno, H., Bonifacino, J.S., and Mellman, I. (1999). A novel clathrin adaptor complex mediates basolateral targeting in polarized epithelial cells. Cell *99*, 189–198.

Folsch, H., Pypaert, M., Maday, S., Pelletier, L., and Mellman, I. (2003). The AP-1A and AP-1B clathrin adaptor complexes define biochemically and functionally distinct membrane domains. J. Cell Biol. *163*, 351–362.

Fukaya, M., Tsujita, M., Yamazaki, M., Kushiya, E., Abe, M., Akashi, K., Natsume, R., Kano, M., Kamiya, H., Watanabe, M., and Sakimura, K. (2006). Abundant distribution of TARP γ-8 in synaptic and extrasynaptic surface of hippocampal neurons and its major role in AMPA receptor expression on spines and dendrites. Eur. J. Neurosci. *24*, 2177–2190.

Gan, Y., McGraw, T.E., and Rodriguez-Boulan, E. (2002). The epithelial-specific adaptor AP1B mediates post-endocytic recycling to the basolateral membrane. Nat. Cell Biol. *4*, 605–609.

Garrido, J.J., Fernandes, F., Giraud, P., Mouret, I., Pasqualini, E., Fache, M.P., Jullien, F., and Dargent, B. (2001). Identification of an axonal determinant in the C-terminus of the sodium channel Na(v)1.2. EMBO J. *20*, 5950–5961.

Gu, C., Jan, Y.N., and Jan, L.Y. (2003). A conserved domain in axonal targeting of Kv1 (Shaker) voltage-gated potassium channels. Science *301*, 646–649.

Hara, T., Nakamura, K., Matsui, M., Yamamoto, A., Nakahara, Y., Suzuki-Migishima, R., Yokoyama, M., Mishima, K., Saito, I., Okano, H., and Mizushima, N. (2006). Suppression of basal autophagy in neural cells causes neurodegenerative disease in mice. Nature *441*, 885–889.

Herskovits, J.S., Burgess, C.C., Obar, R.A., and Vallee, R.B. (1993). Effects of mutant rat dynamin on endocytosis. J. Cell Biol. *122*, 565–578.

Hirai, H., Pang, Z., Bao, D., Miyazaki, T., Li, L., Miura, E., Parris, J., Rong, Y., Watanabe, M., Yuzaki, M., and Morgan, J.I. (2005). Nat. Neurosci. Cbln1 is essential for synaptic integrity and plasticity in the cerebellum *8*, 1534–1541.

Horton, A.C., and Ehlers, M.D. (2003). Neuronal polarity and trafficking. Neuron *40*, 277–295.

Inamura, M., Itakura, M., Okamoto, H., Hoka, S., Mizoguchi, A., Fukazawa, Y., Shigemoto, R., Yamamori, S., and Takahashi, M. (2006). Differential localization and regulation of stargazin-like protein, gamma-8 and stargazin in the plasma membrane of hippocampal and cortical neurons. Neurosci. Res. *55*, 45–53.

Jareb, M., and Banker, G. (1998). The polarized sorting of membrane proteins expressed in cultured hippocampal neurons using viral vectors. Neuron *20*, 855–867.

Kantheti, P., Qiao, X., Diaz, M.E., Peden, A.A., Meyer, G.E., Carskadon, S.L., Kapfhamer, D., Sufalko, D., Robinson, M.S., Noebels, J.L., and Burmeister, M. (1998). Mutation in AP-3 delta in the mocha mouse links endosomal transport to storage deficiency in platelets, melanosomes, and synaptic vesicles. Neuron *21*, 111–122.

Lee, C.J., Bardoni, R., Tong, C.K., Engelman, H.S., Joseph, D.J., Magherini, P.C., and MacDermott, A.B. (2002). Functional expression of AMPA receptors on central terminals of rat dorsal root ganglion neurons and presynaptic inhibition of glutamate release. Neuron *35*, 135–146.

Lu, C.R., Hwang, S.J., Phend, K.D., Rustioni, A., and Valtschanoff, J.G. (2002). Primary afferent terminals in spinal cord express presynaptic AMPA receptors. J. Neurosci. *22*, 9522–9529.

Madrid, R., Le Maout, S., Barrault, M.B., Janvier, K., Benichou, S., and Merot, J. (2001). Polarized trafficking and surface expression of the AQP4 water channel are coordinated by serial and regulated interactions with different clathrin-adaptor complexes. EMBO J. *20*, 7008–7021.

Matsuda, S., Launey, T., Mikawa, S., and Hirai, H. (2000). Disruption of AMPA receptor GluR2 clusters following long-term depression induction in cerebellar Purkinje neurons. EMBO J. *19*, 2765–2774.

Matsuda, S., Matsuda, K., and Yuzaki, M. (2006). A new motif necessary and sufficient for stable localization of the delta2 glutamate receptors at postsynaptic spines. J. Biol. Chem. *281*, 17501–17509.

Mitsui, S., Saito, M., Hayashi, K., Mori, K., and Yoshihara, Y. (2005). A novel phenylalanine-based targeting signal directs telencephalin to neuronal dendrites. J. Neurosci. *25*, 1122–1131.

Mizushima, N., Yamamoto, A., Matsui, M., Yoshimori, T., and Ohsumi, Y. (2004). In vivo analysis of autophagy in response to nutrient starvation using transgenic mice expressing a fluorescent autophagosome marker. Mol. Biol. Cell *15*, 1101–1111.

Nicoll, R.A., Tomita, S., and Bredt, D.S. (2006). Auxiliary subunits assist AMPA-type glutamate receptors. Science *311*, 1253–1256.

Nishiyama, J., Miura, E., Mizushima, N., Watanabe, M., and Yuzaki, M. (2007). Aberrant membranes and double-membrane structures accumulate in the axons of Atg5-null Purkinje cells before neuronal death. Autophagy *3*, 591–596.

Poyatos, I., Ruberti, F., Martinez-Maza, R., Gimenez, C., Dotti, C.G., and Zafra, F. (2000). Polarized distribution of glycine transporter isoforms in epithelial and neuronal cells. Mol. Cell. Neurosci. *15*, 99–111.

Rivera, J.F., Ahmad, S., Quick, M.W., Liman, E.R., and Arnold, D.B. (2003). An evolutionarily conserved dileucine motif in Shal K+ channels mediates dendritic targeting. Nat. Neurosci. *6*, 243–250.

Rodriguez-Boulan, E., and Musch, A. (2005). Protein sorting in the Golgi complex: shifting paradigms. Biochim. Biophys. Acta *1744*, 455–464.

Ruberti, F., and Dotti, C.G. (2000). Involvement of the proximal C terminus of the AMPA receptor subunit GluR1 in dendritic sorting. J. Neurosci. *20*, RC78.

Sampo, B., Kaech, S., Kunz, S., and Banker, G. (2003). Two distinct mechanisms target membrane proteins to the axonal surface. Neuron *37*, 611–624.

Silverman, M.A., Peck, R., Glover, G., He, C., Carlin, C., and Banker, G. (2005). Motifs that mediate dendritic targeting in hippocampal neurons: a comparison with basolateral targeting signals. Mol. Cell. Neurosci. *29*, 173–180.

Simmen, T., Honing, S., Icking, A., Tikkanen, R., and Hunziker, W. (2002). AP-4 binds basolateral signals and participates in basolateral sorting in epithelial MDCK cells. Nat. Cell Biol. *4*, 154–159.

Takago, H., Nakamura, Y., and Takahashi, T. (2005). G protein-dependent presynaptic inhibition mediated by AMPA receptors at the calyx of Held. Proc. Natl. Acad. Sci. USA *102*, 7368–7373.

Tanaka, J., Nakagawa, S., Kushiya, E., Yamasaki, M., Fukaya, M., Iwanaga, T., Simon, M.I., Sakimura, K., Kano, M., and Watanabe, M. (2000). Gq protein alpha subunits Galphaq and Galpha11 are localized at postsynaptic extrajunctional membrane of cerebellar Purkinje cells and hippocampal pyramidal cells. Eur. J. Neurosci. *12*, 781–792.

Tashiro, A., Dunaevsky, A., Blazeski, R., Mason, C.A., and Yuste, R. (2003). Bidirectional regulation of hippocampal mossy fiber filopodial motility by kainate receptors: a two-step model of synaptogenesis. Neuron *38*, 773–784.

Tomita, S., Chen, L., Kawasaki, Y., Petralia, R.S., Wenthold, R.J., Nicoll, R.A., and Bredt, D.S. (2003). Functional studies and distribution define a family of transmembrane AMPA receptor regulatory proteins. J. Cell Biol. *161*, 805–816.

Tomita, S., Fukata, M., Nicoll, R.A., and Bredt, D.S. (2004). Dynamic interaction of stargazin-like TARPs with cycling AMPA receptors at synapses. Science *303*, 1508–1511.

Tomita, S., Adesnik, H., Sekiguchi, M., Zhang, W., Wada, K., Howe, J.R., Nicoll, R.A., and Bredt, D.S. (2005a). Stargazin modulates AMPA receptor gating and trafficking by distinct domains. Nature *435*, 1052–1058.

Tomita, S., Stein, V., Stocker, T.J., Nicoll, R.A., and Bredt, D.S. (2005b). Bidirectional synaptic plasticity regulated by phosphorylation of stargazin-like TARPs. Neuron *45*, 269–277.

Uchigashima, M., Fukaya, M., Watanabe, M., and Kamiya, H. (2007). Evidence against GABA release from glutamatergic mossy fiber terminals in the developing hippocampus. J. Neurosci. *27*, 8088–8100.

Vandenberghe, W., Nicoll, R.A., and Bredt, D.S. (2005). Stargazin is an AMPA receptor auxiliary subunit. Proc. Natl. Acad. Sci. USA *102*, 485–490.

Wang, Q.J., Ding, Y., Kohtz, D.S., Mizushima, N., Cristea, I.M., Rout, M.P., Chait, B.T., Zhong, Y., Heintz, N., and Yue, Z. (2006). Induction of autophagy in axonal dystrophy and degeneration. J. Neurosci. *26*, 8057–8068.

Yap, C.C., Murate, M., Kishigami, S., Muto, Y., Kishida, H., Hashikawa, T., and Yano, R. (2003). Adaptor protein complex-4 (AP-4) is expressed in the central nervous system neurons and interacts with glutamate receptor delta2. Mol. Cell. Neurosci. *24*, 283–295.